

On the effect of deep-rolling and laser-peening on the stress-controlled low- and high-cycle fatigue behavior of Ti-6Al-4V at elevated temperatures up to 550°C

I. Altenberger^{1*}, R. K. Nalla^{2*}, Y. Sano³, L. Wagner⁴, R. O. Ritchie⁵

¹ *Wieland-Werke AG, Ulm, Germany*

² *LensVector Inc., Mountain View, USA*

³ *Toshiba Corporation, Yokohama, Japan*

⁴ *Clausthal University of Technology, Clausthal, Germany*

⁵ *Materials Sciences Division, Lawrence Berkeley Laboratory, and Department of Materials Science and Engineering, University of California, Berkeley, CA, USA*

ABSTRACT

The effect of surface treatment on the stress/life fatigue behavior of a titanium Ti-6Al-4V turbine fan blade alloy is investigated in the regime of 10^2 to 10^6 cycles to failure under fully reversed stress-controlled isothermal push-pull loading between 25° and 550°C at a frequency of 5 Hz. Specifically, the fatigue behavior was examined in specimens in the deep-rolled and laser-shock peened surface conditions, and compared to results on samples in the untreated (machined and stress annealed) condition. Although the fatigue resistance of the Ti-6Al-4V alloy declined with increasing test temperature regardless of surface condition, deep-rolling and laser-shock peening surface treatments were found to extend the fatigue lives by factors of more than 30 and 5-10, respectively, in the high-cycle and low-cycle fatigue regimes at temperatures as high as 550°C. At these temperatures, compressive residual stresses are essentially relaxed; however, it is the presence of near-surface work hardened layers, with a nanocrystalline structure in the case of deep-rolling and dense dislocation tangles in the case of laser-shock peening, which remain fairly stable even after cycling at 450°-550°C, that provide the basis for the beneficial role of mechanical surface treatments on the fatigue strength of Ti-6Al-4V at elevated temperatures.

Keywords: Fatigue; Titanium alloys; Surface treatments; Deep-rolling; Laser shock peening

1. Introduction

Compressor fan blades and disks in aircraft jet propulsion engines are commonly made from titanium alloys, *e.g.*, Ti-6Al-4V, due to their favorable combination of low density with strength, fatigue, oxidation and wear resistance. In service, these alloys experience severe mechanical and thermal loading conditions, in particular high- and low-cycle fatigue cycles resulting, respectively, from high frequency vibrations in flight and start and stop cycles of the engine during take-off and landings [1]. To assess the fatigue properties for these applications, constant amplitude fatigue testing is routinely carried out at ambient to elevated temperatures under stress, total strain or plastic strain control in order to discern the cyclic softening or hardening behavior as a function of fatigue cycles and the number of cycles to failure. To affect this softening/hardening behavior and enhance fatigue lives, mechanical surface treatments are often utilized, both to impart compressive residual stresses and to develop sufficiently deep work-hardened regions in the surface layers. With such procedures, which have traditionally involved shot peening, significant increases in the fatigue lives of many metallic materials can be realized [2-6].

However, there are other surface treatments in addition to shot peening [7] that have been used to increase resistance to early fatigue crack initiation and growth in metallic structures, notably deep-rolling [8], roller-burnishing [9] or low-plasticity burnishing¹ [10], and laser-shock (or laser) peening

* formerly at the Materials Sciences Division, Lawrence Berkeley National Laboratory, Berkeley, USA

¹ The terminology "deep rolling" refers to a surface rolling treatment using rolls or ball-point tools for the purpose of inducing deep plastic deformations and compressive residual stresses in near-surface regions, in contrast to "roller

[11-14]. Shot peening, with or without subsequent polishing, has been utilized now for decades to induce favorable near-surface microstructures and compressive residual stress states [15,16], although several recent studies have revealed the superiority of the so-called alternative surface treatments [8]. Specifically, laser-shock peening² has proven to be a particularly effective surface treatment for both α - β - and near- β -titanium alloys, especially for fan blade applications [17,18].

There is considerable information in the literature on the effects of shot peening on the fatigue performance of Ti-6Al-4V alloys at room temperature, *e.g.* refs. [7,19]. The procedure is known to improve the fatigue strength of Ti-6Al-4V in both the high-cycle fatigue (HCF) and low cycle fatigue (LCF) regimes [20]. However, the response to surface treatments depends significantly on the microstructure and/or heat treatment [7,15]. For example, compared to electropolished material, air cooled duplex microstructures (comprising primary α -grains embedded in a lamellar (α + β) matrix) appear to exhibit little improvement in the HCF-strength after shot-peening, whereas water quenched lamellar duplex microstructures show a pronounced improvement, a finding that has been related to the differing mean stress sensitivity of the two structures as sub-surface cracking due to tensile residual stresses was assumed to be the dominant crack initiation mechanism [16]. Presently, shot peening is still the most used mechanical surface treatment in the turbine engine industry, although the associated surface roughening is known to be problematic since it reduces the gas flow efficiency and can severely reduce the crack initiation phase. To counter this roughness effect, either an additional polishing step or the use of alternative mechanical surface treatments such as laser-shock peening or deep rolling have been tried; indeed these alternative approaches to simple shot peening have become increasingly popular over the past decade [8,11,18].

Most studies on the fatigue resistance of deep-rolled and laser-shock peened Ti-6Al-4V alloys have focused on the LCF regime [18] and considered the issues of the near-surface residual stresses [11,21] and surface microstructures induced by the mechanical surface treatment [22]. One question is the effectiveness of these surface treatments for applications that required higher temperature service. Indeed, by varying temperature (only) up to 550-600°C, it has been shown that the residual stresses are essentially annealed out in Ti-6Al-4V, whereas the highly work-hardened nanoscale surface microstructures tend to be much more thermally stable and still effective [22]. However, few studies have considered the effects of both cyclic plasticity and temperature on the stability and effect of the residual stresses and work-hardened surface layers during elevated temperature fatigue.

Accordingly, it is the aim of this work to show systematically the limits of cyclic deformation and temperatures where mechanical surface treatments can remain an effective method of fatigue strength enhancement in Ti-6Al-4V and further to discern the salient microstructural mechanisms underlying such behavior. The ultimate objective is to develop a tailored microstructure-based approach of surface engineering for enhancing structural integrity in these alloys.

2. Experimental Procedures

The Ti-6Al-4V alloy under study was received as 2-m long, 14-mm diameter cylindrical bars from Hempel Company, Germany, with a composition (in wt.%) of 6.22% Al, 4.01% V, 0.2% Fe, 0.2% O, 0.02% C, 0.01% N, 0.001% H, balance Ti. The material was solution heat treated at 970°C for 30 min and subsequently air cooled. After machining, 7-mm diameter cylindrical specimens, with a 15-mm gauge length, were stress relieved at 700°C in an argon atmosphere. The resulting bimodal microstructure consisted of interconnected equiaxed primary α -grains and α + β colonies (transformed β); the volume content of the primary α -phase was 37 %, as measured by image analysis. An optical micrograph of the bimodal microstructure (etched in Kroll solution) is shown in Fig. 1. Room

burnishing" which is usually applied with lower forces or pressures and mostly aims to obtain a certain surface quality, especially in terms of minimized roughness (in addition to inducing residual stress). "Low plasticity burnishing" generally refers to a mechanical surface treatment (sometimes using low or moderate forces/pressures as compared to "deep rolling") with rolls or ball-point tools [8,9,10].

² Laser-shock peening is a mechanical surface treatment using pulsed lasers. The laser-illuminated component which is strengthened by laser peening is covered by water. After the shock-wave propagation, the surface is elastically constrained to form a compressive residual stress. The process can be carried out with or without sacrificial coating (but with different pulse energies).

1 temperature tensile tests gave yield and ultimate tensile strengths of 968 and 1030 MPa, respectively,
2 with an elongation of 29%, similar to the properties of the Ti-6Al-4V alloy studied in our previous
3 work on surface treatments [18,22-26]. The average grain size was $\sim 15 \mu\text{m}$ after heat treatment.

4 Surface roughness was measured using a mechanical sensor ("Perthometer" by Mahr Company,
5 Göttingen, Germany) for all surface conditions to characterize the average roughness depth, R_z , which
6 is a 10-point average distance between the five highest peaks and five deepest valleys within the
7 sampling length from the roughness profile. The measured roughness values R_z were: $1.8 \mu\text{m}$ for the
8 untreated condition, $0.7 \mu\text{m}$ for the deep rolled condition, $2.1 \mu\text{m}$ for the laser peened condition with a
9 coating and $15 \mu\text{m}$ for the laser peened condition without a coating.

10 The fatigue properties of the untreated (annealed) material were compared to surface treated
11 specimens subjected to either deep-rolling or laser-shock peening. Deep-rolling was performed with a
12 so-called ball-point rolling device, using a hydrostatic spherical rolling element (6.6-mm diameter)
13 with a constant feed of 0.1125 mm per revolution and a rolling pressure of 150 bar (rolling force of 0.5
14 kN). The main feature of the ball-point deep-rolling device is the burnishing ball which is
15 hydrostatically suspended by pressurized liquid, either oil or water soluble coolant. The hard ball is
16 pressed with controllable operating pressure against the work piece and can move freely while the
17 work-piece is rotated. This treatment is akin to lathe machining with a hydrostatically-seated spherical
18 rolling element instead of the cutting tool.

19 Laser-shock peening was carried out in two principal variants: the first without the use of a coating
20 on the sample and the second with black paint as sacrificial coating. For the first method without a
21 coating, a Q-switched frequency doubled Nd:YAG-laser (wavelength 532 nm), with a spot size of 0.8
22 mm (which can be variable), a power density of 5 GW/cm² and a coverage of 36 shots/mm² (1800%
23 for an illumination diameter of 0.8 mm), was used, as described in detail elsewhere [27]. For the
24 second approach with a coating, a Nd:Glass-laser (wavelength 1064 nm) was used, with a spot size of
25 2x2mm², a power density of 10 GW/cm² and a coverage of 200%.

26 Stress-life fatigue testing on both untreated and surface treated material was carried out using
27 smooth-bar cylindrical specimens, cycled in tension-compression under load control, on a 160kN-
28 servo-hydraulic testing machine (Carl Schenck AG, Darmstadt) with a load ratio (minimum to
29 maximum loads) of $R = -1$; a test frequency of $\nu = 5 \text{ Hz}$ (sine wave) was employed with varying stress
30 amplitudes to give fatigue lives between 10^3 and 10^6 cycles. Specimens were tested in room air at
31 temperatures between 22° and 550°C, the elevated temperatures being achieved by *in situ* heating in a
32 small thermostatically-controlled furnace. Before starting the fatigue tests, the specimens were
33 equilibrated at temperature for ~ 10 min. During fatigue cycling, the axial strain (for generating the
34 cyclic softening/hardening curves) was monitored using a capacitive extensometer. The resolution of
35 the capacitive extensometer was in the range of $5 \mu\text{m}$. Data are presented in the form of Wöhler (S/N)
36 curves of the applied stress amplitude S as a function of the numbers of cycles to failure (N_f). The S/N
37 data and the data for generating cyclic softening/hardening curves originated from the same tests and
38 samples. The plastic strain amplitudes in the stress-controlled cyclic deformation curves (Fig. 5) were
39 determined in the following way: During the fatigue tests extensions (measured by the capacitive
40 extensometer) and forces (measured by the load cell) were registered every 10 ms and full force-
41 extension hysteresis loops were recorded after 1, 5, 10, 20, 50, 60, 80, 100, 200, 300, 400, 600, 1000 ,
42 2000, 3000, 4000, 6000, 7000, 10000, 15000, 30000, 50000, 700000 and 100000 cycles by the
43 software (a recording of every single cycle was not carried out due to a lack of memory capacity of the
44 computer hardware). These force-extension hysteresis loops were converted into stress-(total) strain
45 hysteresis loops by dividing the force by the initial cross section of the specimen and by dividing the
46 extension by the gauge length. A correction of the cross section area during the fatigue test was not
47 carried out. The plastic strain amplitudes of the fatigue cycles mentioned above were then determined
48 as the half-widths of the hysteresis loops (half of the plastic strain range) at zero stress. For generating
49 the Manson-Coffin plot, plastic strain amplitudes were taken from $0.9N_f$ (N_f = number of cycles to
50 fracture) instead of (the more common practice) $0.5N_f$. This was done because for our data this
51 procedure generally gave better linear regressions (in the double logarithmic Manson-Coffin plot) than
52 values taken at $0.5N_f$. This is possibly due to a more "saturated" or stable dislocation arrangement at
53 $0.9N_f$, as compared to $0.5N_f$. In all cases, care was taken that no data were used from the cyclic
54 deformation curve from a stage where macro crack propagation had already occurred.

1 To characterize the nature of the microstructure in the mechanically treated surface layers,
2 transmission electron microscopy (TEM) was performed with a Philips CM 200 microscope at an
3 acceleration voltage of 200 kV. Plan view TEM foils (parallel to the stress axis of the fatigue tests) at
4 two different depths below the surface (0-2 μm , termed “surface”; 4-6 μm , termed “subsurface”) were
5 generated by a combination of twin and single jet-polishing at a temperature of -15°C using a
6 perchloric acid/ethanol electrolyte. Usually bright-field images were recorded under two-beam
7 conditions. Corresponding fracture surfaces were examined with scanning electron microscopy using
8 secondary electron imaging.

9 Residual stresses were determined by standard x-ray diffraction techniques using line shifts of x-
10 ray diffraction peaks. Lattice strain measurements were performed using CrK_α radiation at the $\{201\}$ -
11 lattice planes of the hexagonal α -phase. To calculate the residual stresses, the $\sin^2\psi$ -method was
12 applied using the Voigt elastic constant $1/2s_2 = (1 + \nu)/E = 12.09 \times 10^{-6} \text{ mm}^2/\text{N}$, where E is Young's
13 modulus and ν is Poisson's ratio [28]. Specifically, linear regression was used to determine the slopes
14 of 2θ vs. $\sin^2\psi$ for stress determination ($\psi =$ tilt angle, $\theta =$ scatter angle for constructive interference
15 (Bragg diffraction³), with a total of 11 ψ angles used for each measurement. The stress state was
16 assumed to be biaxial, with the bulk of information of the diffracted x-ray originating from the surface.
17 All residual stresses and “full width at half maximum” (FWHM) values were measured in longitudinal
18 direction of the specimens. A collimator with a diameter of 1 mm was used for illuminating the
19 specimens.
20
21
22

23 3. Results and Discussion

24 3.1. Microstructure of the near-surface layers

25 The near-surface microstructures of the untreated, deep-rolled and laser-shock peened (without
26 coating) conditions are shown in Fig. 2 prior to fatigue testing. In the untreated condition, a dislocation
27 density of 10^8 - 10^9 cm^{-2} was present within the α -phase, although dislocation densities were somewhat
28 higher close to the interface between α -phase and β -lamellae.
29
30
31
32

33 In the deep rolled condition the deep-rolling process induced a thin (1-2 μm) nanocrystalline
34 surface layer by the severe plastic surface deformation (SPD) in the direct surface regions. The
35 crystallite sizes were about 50 nm directly at the surface. Due to the formation of high-angle grain
36 boundaries, a strong orientation contrast between the crystallites occurs. Similar to deep-rolled
37 austenitic steels [29], the nanocrystallites exhibit a complex lamellar substructure, possibly caused by
38 high elastic strain and/or internal twinning. In contrast to the steel, the grains size distribution is
39 broader and resembles the nanostructure in the first stages of nanocrystallization of ball milled metals
40 [30]. At greater depths ($> 2 \mu\text{m}$) in the deep-rolled condition, high dislocation densities similar to the
41 direct surface microstructure of the laser-shock peened condition were observed.
42
43
44

45 A different microstructure is observed after laser-shock peening: here, no nanocrystallites were
46 formed, but the dislocation arrangement consisted of diffuse tangled and debris-like structures, cell
47 formation was not observed, the dislocation arrangement was almost entirely planar.

48 Both laser-shock-peening and deep-rolling led to a significant increase in the near-surface
49 dislocation density of the α -phase in the range of 10^{11} cm^{-2} . Both laser-shock peening and deep-rolling
50 increased the microhardness from ~ 300 - 320 VPN to 375 - 400 VPN , with the increase being somewhat
51 more pronounced in the deep-rolled condition.
52

53 Compressive residual stresses of ~ 600 - 700 MPa were measured at the surface after both surface
54 treatments. The work-hardened zone (mechanically hardened “case”) extended about 1 mm into depth
55 for deep-rolling and 0.9 mm into depth for laser-shock peening.
56
57
58
59

60 ³ The angle between an incident x-ray beam and a set of crystal planes for which the secondary radiation displays a maximum
61 intensity as a result of constructive interference
62
63
64
65

3.2. Effect of mechanical surface treatments on the fatigue life of Ti-6Al-4V at 22°C

1
2 The stress/life S/N fatigue behavior of Ti-6Al-4V is plotted in Fig. 3 in terms of the stress
3 amplitude σ_a as a function of number of cycles N_f to failure (at $R = -1$, 5 Hz frequency) for the deep-
4 rolled and laser-shock peened structures, as compared to the untreated structure, at 22°C. At room
5 temperature, it is apparent that deep-rolling and laser-shock peening can increase the fatigue
6 endurance strength at 10^6 to 10^7 cycles by some 25% or more, *i.e.*, the endurance strengths under pure
7 tension-compression loading⁴ are more than 100 MPa higher after mechanical surface treatment. It
8 should be noted from this figure that laser-shock peening performed without coating generally yielded
9 higher fatigue strengths and/or higher cycles to failure than peening with coating; this is not
10 necessarily a general trend for all materials, however, as similar studies [32] on AISI 304 stainless
11 steel showed no noticeable effect on fatigue lives whether or not a coating was used.
12

13 For the untreated condition, the data in Fig. 3 reveal a fatigue strength of 380-400 MPa for Ti-6Al-
14 4V at room temperature, which in good agreement with other studies [33] which reported fatigue
15 endurance strengths of ~ 380 MPa ($R = -1$) for cycle counts out to 10^8 or 10^9 cycles.
16

17 It should be noted that the fatigue strength values of 380 and 480 MPa in Fig. 3 for, respectively,
18 the untreated and mechanically surface treated conditions correspond to just one unbroken specimen
19 per treatment and were not obtained through a staircase method. Hence great care has to be taken
20 while interpreting these non-statistically evaluated S/N curves.
21
22
23

3.3. Effect of mechanical surface treatments on the fatigue life of Ti-6Al-4V at elevated temperatures

24 Corresponding S/N curves for behavior at 250°C, 350°C 450°C and 650°C are shown in Fig. 4. At
25 250°C, it is apparent that although the fatigue strength has generally decreased compared to room
26 temperature behavior, the mechanical surface treatments still have a significant effect in enhancing the
27 fatigue strength. Specifically, compared to the untreated condition, both deep-rolling and laser-shock
28 peening increased the 10^6 -cycle fatigue strength by well over 25% (~ 100 MPa). A similar picture can
29 be observed at test temperatures of 350°C, 450°C and 550°C (Figs. 4b-d respectively), although the
30 elevation in the 10^6 cycles fatigue strength from the mechanical surface treatments is progressively
31 decreased to ~ 50 MPa at 350°-550°C (which corresponds to a fatigue strength increase of 10-15%).
32 The beneficial influence of mechanical surface treatments on the fatigue life is also prevalent in the
33 low cycle fatigue (LCF) regime at lifetimes less than 5×10^4 cycles, although the effect is reduced to
34 near zero for lifetimes shorter than $\sim 10^3$ cycles. This is attributed to instability of near-surface work
35 hardening, microstructures and compressive residual stresses, as noted elsewhere [11,34-38]. At all
36 temperatures, except for 550°C, deep-rolling treatments provide slightly superior, or at least
37 equivalent, improvements in fatigue lifetimes compared to laser-shock peening (performed using a
38 surface coating). At 250°-450°C, laser-shock peening (without coating) is also capable of producing at
39 least as high fatigue lives as deep-rolling, although with only limited data available, it is not as yet
40 clear whether this represents a general trend.
41
42
43
44
45

46 The cyclic deformation behavior of the untreated and deep-rolled material conditions at 250° and
47 350°C are shown in Fig. 5. Room temperature behavior in the untreated Ti-6Al-4V was qualitatively
48 similar to that reported previously [39], namely slight cyclic softening with increasing number of
49 cycles. Cyclic deformation curves (plastic strain amplitude ε_{ap} vs. number of cycles N) for the
50 untreated and deep-rolled conditions were similar in shape, although levels of strain were different; the
51 laser-shock peened samples, conversely, often exhibited earlier cyclic softening [18]. Principally, three
52 types of cyclic deformation curves were observed: (i) Generally, at high mechanical or thermal loading
53 ($\sigma_a > 500$ -550 MPa at 250°C and 350°C or $\sigma_a > 430$ MPa at 550°C), *i.e.*, at shorter lives in the LCF
54 regime, monotonic cyclic softening was observed; (ii) Conversely, at low stress amplitudes or
55 temperatures, *i.e.*, at longer lives in the HCF regime, no pronounced softening could be seen ($\sigma_a < 460$
56 MPa at 350°C or up to $\sigma_a = 800$ MPa at below 250°C); (iii) Between these two extremes at medium
57
58
59

60
61 ⁴ The increase in fatigue strength from surface treatment has been reported to be even more pronounced for samples tested in
62 rotary bending or in pure bending [11,31].
63
64
65

1 stress amplitudes or temperatures ($460 \text{ MPa} < \sigma_a < 540 \text{ MPa}$ at 350°C), cyclic softening was typically
2 followed by cyclic hardening over the majority of the fatigue life until macrocrack propagation and
3 fracture intervened. In all cases, higher stress amplitudes and temperatures led to higher plastic strain
4 amplitudes.

5 It is evident from Fig. 5 that the cyclic deformation behavior (under stress control) of untreated
6 and deep-rolled Ti-6Al-4V changes with rising temperature in the range 250° to 350°C from one of
7 monotonic cyclic softening, *i.e.* an increase of the plastic strain amplitude with increasing number of
8 cycles) to cyclic softening followed by cyclic hardening. This observation is consistent to previous
9 studies on Ti-6Al-4V [40-42], which showed that at 350°C cyclic softening was followed by cyclic
10 hardening for low strain amplitudes whereas monotonic cyclic softening occurred at high strain
11 amplitudes, with no saturation in cyclic hardening apparent [9].
12

13 With respect to the LCF-regime, a Manson-Coffin-plot of the plastic strain amplitude as a function
14 of the number of cycles to failure for both the untreated and deep-rolled Ti-6Al-4V alloys is shown in
15 Fig. 6. It is apparent that the Manson-Coffin behavior is not strongly dependent on temperature.
16 Specifically, Manson-Coffin exponents (*i.e.*, slope of the plot (Table 1) were significantly but not
17 drastically different between 250° and 550°C (room temperature: -0.76 ; even at 550°C it only
18 increased to -0.96). At high homologous temperatures, Manson-Coffin exponents of metallic alloys
19 can become highly temperature-dependent where creep effects become significant [43], in contrast to
20 lower homologous temperatures where this is not generally the case [44]. The former is often
21 characterized by a transition from fatigue-dominated to creep-dominated failure [45] with a
22 consequent change in mechanism to intergranular failure; no such phenomena were apparent with the
23 current materials where crack paths were primarily transgranular. However, it should be noted that at
24 very high stress amplitudes and high temperatures, pronounced *cyclic* creep occurs, *i.e.*, a total mean
25 strain of $\sim 2\%$ at $\sigma_a = 600 \text{ MPa}$ at 250°C or at $\sigma_a = 430 \text{ MPa}$ at 550°C . The data from total strain
26 control were taken from ref. [40]. There, the experimental conditions were notably different (apart
27 from the control mode) from those in our experiments. More specifically, the temperature was 350°C
28 and the strain rate was 10^{-3} s^{-1} or smaller (and therefore by a factor of roughly 10 smaller than in our
29 tests). In addition, the environmental atmosphere was vacuum and not air. We are well aware, that
30 these test conditions are significantly different from our stress-controlled tests. The Manson-Coffin
31 plot from the data resulting from total strain control experiments at 350°C /vacuum also used plastic
32 strain amplitudes at $0.5N_f$ (data from ref. [40]). Nevertheless, it shows that despite these different
33 conditions, an approximately similar Manson-Coffin plot can be derived, although the slopes are
34 somewhat different (Table 1).
35
36
37

38 In general though, exponents were closer to -0.5 for the deep-rolled structures, as compared to -0.8
39 for the untreated structures. The intersecting point is around 2×10^3 cycles in the LCF regime,
40 meaning that for lives in excess of this, the deep-rolled Ti-6Al-4V structures will exhibit progressively
41 longer lives than the untreated structures at a given stress amplitude. We can conclude from this that
42 the process of deep-rolling is beneficial to fatigue lives in Ti-6Al-4V in both the LCF and HCF
43 regimes, and that this benefit increases with longer lives. No hints for pronounced dynamic strain
44 aging were observed in our tests, even at 250°C .⁵
45
46

47 The different fatigue results from the various surface conditions are clearly not just a consequence
48 of the different surface roughness values. Although the deep-rolled condition shows a significantly
49 lower surface roughness than the untreated material, the laser-peened conditions (and here especially
50 the laser-peened condition without coating) exhibit a pronounced micro-topography and increased
51 surface roughness. In spite of the increased roughness, however, both the laser-peened conditions
52 show cyclic lifetimes which are comparable or sometimes even superior to the fatigue lives of the
53 deep-rolled condition. In practice, it is very difficult to delineate the effect of surface roughness on the
54 fatigue life and strength in mechanically surface treated materials from other effects. To clearly
55 separate the effect of surface roughness from other factors the study would require identical
56 microstructures (at and closely beneath the surface), identical residual stress and texture states,
57 identical damage mechanisms and identical "case" depths of the different surface treatments.
58
59

60
61 ⁵ It is assumed that significant dynamic strain aging does not occur due to an unfavorable combination of strain rate and
62 temperature. At 5 Hz, the strain rates were typically as high as $d\varepsilon/dt \sim 10^{-2}$.
63
64
65

1 In addition to the nanocrystalline surface zone in the deep-rolled surface state, the different surface
2 roughnesses in the various mechanically surface treated conditions have to be taken into account,
3 especially in the HCF regime, where crack initiation consumes the greater part of fatigue life. In this
4 study the density of the surface crack initiation sites was not investigated systematically. However, in
5 general it was found that after deep rolling the crack density was lower than after laser (shock)
6 peening, which in part is possibly due to the lower surface roughness of the deep-rolled condition as
7 compared to the laser-peened ones, leading to a reduced number of local stress raisers. For fatigue
8 tests at room temperature under rotary bending, it was shown that early crack initiation in laser-peened
9 samples as compared to deep-rolled ones can be significantly delayed by a subsequent mechanical
10 polishing after laser peening [20]. Although the effects of the coating on the fatigue crack density were
11 not investigated in our studies, laser peening without a coating resulted in higher surface roughness
12 values than laser peening with coating. It is interesting, that despite this higher surface roughness, the
13 laser-peening treatment without a coating resulted in higher fatigue lives than the laser-shock peening
14 with a coating, suggesting that the role of the differing surface roughnesses in this study were
15 secondary to the more significant role of near-surface work hardening and residual stress states.
16

17 From shot peening, it is known that the detrimental effect of increased surface roughness and even
18 microcracks can be compensated by compressive residual stress fields as well as by cold work through
19 impeding the growth of microcracks. We presume that a similar effect takes place in the mechanically
20 surface treated Ti-6Al-4V investigated here. In our study, although the presence of highly work-
21 hardened layers with their nanocrystalline structure, as well as the compressive residual stresses (at
22 temperatures below 450°C) appear to have a more pronounced effect on the fatigue life of Ti-6Al-4V,
23 this should not imply that the role of surface roughness is unimportant; optimizing the surface
24 topography should not be neglected since Ti-6Al-4V alloys are known to be highly notch-sensitive at
25 room and elevated temperatures, as is apparent from their known susceptibility to foreign object
26 damage [23].
27
28

29 *3.4. Effect of high-temperature fatigue on near-surface microstructure*

30
31 To examine the nature of the work-hardened surface layer for the deep-rolled surface condition,
32 TEM characterization was performed after fatiguing for 2×10^3 cycles at a stress amplitude of 430
33 MPa at 200°C and at 400°C, the objective being to investigate whether combined (iso)thermal and
34 cyclic mechanical loading affects near-surface microstructures (Fig. 7). In contrast to laser-shock
35 peening, deep-rolling induced a nanocrystalline surface layer with a region of dense dislocation
36 tangles below (see also Fig. 2). The nanocrystalline surface layer had an average grain size of ~50 nm;
37 in the subsurface region some 5-10 μm below this, the microstructure was characterized by regions of
38 heavily tangled dislocations (with a dislocation density of $\sim 10^{11} \text{ cm}^{-2}$). The nanocrystalline surface
39 layer in Ti-6Al-4V was found to remain stable after high-temperature cycling at 200°C and at 400°C.
40 Neither significant grain coarsening nor cracking was observed in this region after 2×10^3 cycles,
41 although it appears that at a depth of 5 to 10 μm a slight decrease of dislocation density was observed
42 at the higher temperature (Fig. 7). Whereas it has been demonstrated that the near-surface
43 microstructures induced by deep-rolling in solution treated and over-aged Ti-6Al-4V are exceedingly
44 stable to temperatures up to at least 650°C *without* mechanical loading [22], the current results indicate
45 that in the presence of mechanical loading from stress-controlled fatigue cycling, these surface layers
46 are similarly stable at temperatures of 200° to 400°C.
47
48
49
50

51 Fig. 8 shows the dislocation arrangements in the corresponding surface and sub-surface regions of
52 Ti-6Al-4V after laser-shock peening (without coating) and cycling in stress-controlled fatigue at a
53 stress amplitude of 460 MPa at 250°C and at 350°C. The sub-surface layer of heavily tangled
54 dislocations again remained fairly stable during fatigue at temperature, akin to the deep-rolled treated
55 material, although there was no evidence of the cell-like dislocation structures that are typically
56 observed for mechanically surface treated steels after stress-controlled fatigue at high plastic strains
57 [29,46]. The similar nature and stability of the subsurface dislocation tangles as well as the similar
58 work-hardened "case depth" in both the laser-shock peened and deep-rolled conditions during
59 isothermal fatigue suggest a possible explanation for the quite similar fatigue lives of both conditions
60 at elevated temperature. However, there is one striking difference between these two microstructures,
61
62
63
64
65

1 and that is the existence of the nanocrystalline surface layer which occurs only in the deep-rolled, but
2 not the laser-shock peened, condition. It is well known that nanocrystalline materials have superior
3 fatigue crack initiation resistance as compared to microcrystalline conditions [47]; consequently, at
4 low and moderate homologous temperatures ($< 0.4 T_m$) this appears to confer an additional lifetime
5 benefit in deep-rolled, as compared to laser-shock peened, structures. However, with increasing
6 temperature (especially above $0.4 T_m$), nanocrystalline materials also show aggravated creep behavior
7 as compared to microcrystalline materials. This may be relevant only in the early crack propagation
8 stage, if a combined creep-fatigue mechanism originating from the surface occurs. Indeed, at 550°C ,
9 the laser-shock peened conditions appear to fare equally well, or even better, in terms of fatigue life
10 improvement compared to the deep rolled condition (see Fig. 4).

11 3.5. Fractographic observations

12 Fatigue cracks in untreated, deep-rolled and laser-shock peened samples all revealed that cracks
13 had initiated at the surface leading to final ductile failure at the center of the specimens; macro-images
14 of representative failed fatigue specimens are shown in Fig. 9. It is significant to note that the
15 untreated samples show far more evidence of multiple surface crack initiation, by almost a factor of
16 two, as revealed by the ridges that emanate from the edge of the fracture surface inwards (these are
17 caused by two separate surface cracks intersecting). This is certainly consistent with the notion that
18 the mechanical surface treatments act to suppress crack initiation (rather than crack growth) and thus
19 have a larger influence of fatigue resistance at long lives, *e.g.*, in the HCF regime. Scanning electron
20 microscopy revealed that fatigue fracture surfaces were characterized by the presence of fatigue
21 striations, as shown in Fig. 9.

22 3.6. Role of near-surface cold-work and residual stresses

23 As noted above, based on results at temperatures up to 550°C , both deep-rolling and laser-shock
24 peening (with or without sacrificial coatings) were found to result in extended fatigue lives at elevated
25 temperature, although the effect was smaller than at 22°C . In previous studies [18], this behavior was
26 reported for loading conditions in the LCF regime; the present study confirms that the beneficial effect
27 of these surface treatments also extends to the HCF regime for lifetimes in excess of 5×10^4 cycles
28 (Fig. 10). Since near-surface work hardening as well as compressive residual stresses are clearly more
29 stable in the lower stress HCF regime [35,36,48,49], the lifetime and fatigue strength improvements
30 are logically superior to those observed at shorter lifetimes.

31 Traditionally, one major effect of mechanical surface treatments in promoting fatigue resistance
32 has been ascribed to the generation of compressive residual stresses. While this is well known to be
33 beneficial in improving fatigue lives, the current data in Fig. 10 do not correlate well with the stability
34 of near-surface compressive residual stresses. Residual stresses, measured using x-ray diffraction, are
35 shown in Fig. 11 for the deep-rolled samples as a function of number of fatigue cycles at temperatures
36 of 25° , 250° , 350° , 450° and 550°C . Prior to cycling these stresses are of the order of -500 to -700
37 MPa. With fatigue cycling though, there is some degree of relaxation at all temperatures; the effect,
38 however, is understandably far more pronounced at the higher temperatures. Specifically, after fatigue
39 cycling at a stress amplitude 460 MPa for half the number of cycles to failure, compressive residual
40 stress values were reduced by a factor of ~ 2 to 7 to less than -200 MPa and -100 MPa, respectively, at
41 450° and 550°C . In spite of such a 75 - 90% relaxation in these stresses at 450 - 550°C , the fatigue lives
42 were still enhanced by mechanical surface treatment (indeed, the 10^7 -cycle fatigue endurance strengths
43 at both temperatures were 50 MPa higher than at 22°C (Figs. 3 and 4)), indicating that the major
44 beneficial effect of deep-rolling and laser-shock peening at these higher temperatures is more
45 associated with the presence of the near-surface work hardened layers, which are thermally stable,
46 than the existence of the compressive residual stress gradients.

47 The stability of these work-hardened surface layers can be confirmed, not simply by the *in situ*
48 [22] and *ex situ* (Figs. 7 and 8) TEM studies, but also using x-ray peak broadening measurements,
49 before and after fatigue cycling to half-life, as a function of temperature. The x-ray peak broadening
50
51
52
53
54
55
56
57
58
59
60
61
62
63
64
65

1 measurements can be expressed by the FWHM values of the Bragg diffraction peaks;⁶ measured data
2 are given in Fig. 12. The observed decrease in the broadening of x-ray diffraction peaks of deep-rolled
3 surface regions fatigued at 550°C suggest that a rearrangement of dislocation structures can take place
4 at temperatures above ~450°C. This may involve the formation of low-energy/low lattice distortion
5 dislocation arrangements resulting from cyclic plasticity as well as by annealing or recovery processes
6 such as dislocation annihilation and formation of low-angle boundaries. The work-hardened layers
7 appear to be fairly stable even after fatigue cycling at the higher temperatures; specifically, at
8 temperatures of 450° and 550°C, FWHM-values decrease only by ~6 and 11%, respectively,
9 confirming the relative stability of these layers to both cyclic deformation and temperature. We
10 believe that it is these work-hardened layers that are the primary origin of the fatigue life enhancement
11 in Ti-6Al-4V at elevated temperatures (up to 550°C) resulting from mechanical surface treatments.

12 Mechanistically such work-hardened layers can promote fatigue resistance by several means;
13 these include (i) reducing the extent of local cyclic plasticity by impeding dislocation movement,
14 which in turn reduces the driving force for crack initiation, (ii) providing a hard, very fine-grained
15 microstructure near the surface which also acts to inhibit crack initiation,⁷ and iii) decreasing the early
16 growth rates of small cracks which initiate at or near the surface [18,52]. Systematic studies on the
17 effect of deep-rolling have shown that increasing rolling pressure leads to more pronounced as well as
18 deeper near-surface work-hardening layers, eventually resulting in higher fatigue strengths [53].
19 Naturally, the compressive residual stresses play an important role too in suppressing crack initiation
20 and early growth [54], but the essential message of the current study is that for higher temperature
21 (~450°-550°C) fatigue behavior in Ti-6Al-4V where the residual stresses have effectively relaxed, it is
22 the more stable work-hardened, nanocrystalline surface layers that provide the main benefit of
23 mechanical surface treatments in enhancing fatigue strength.

24 4. Summary and Conclusions

25 Based on an experimental study of the effects of mechanical surface treatments, specifically deep-
26 rolling rolling and laser-shock peening (with and without coating), on the stress-controlled high- and
27 low-cycle fatigue behavior of Ti-6Al-4V (bimodal microstructure) at temperatures of 22°C to 550°C,
28 the following conclusions can be made:

- 29 1. Ti-6Al-4V cyclically softened during fatigue cycling at room temperature. At elevated temperatures,
30 the shape of all cyclic deformation curves depend strongly on the temperature. With increasing
31 temperature or stress amplitude the plastic strain amplitude increased. At $T > 250^{\circ}\text{C}$, at medium stress
32 amplitudes (*e.g.*, $\sigma_a \sim 500$ MPa), cyclic softening was followed by cyclic hardening until fracture.
- 33 2. All surface treatments significantly improved the fatigue endurance strength as well as the fatigue
34 life in the LCF-regime in the temperature range 22°C to 550°C. With increasing temperature, the
35 beneficial effect on fatigue lifetimes was progressively lessened due to relaxation of compressive
36 residual stresses and the much slower degradation of the near-surface work-hardened layers.
- 37 3. Residual stress measurements in the deep-rolled and laser-peened samples as a function of
38 temperature and number of cycles revealed that the stress relaxation follows a logarithmic cycle
39 dependent law. Although macroscopic residual stresses at the surface decreased drastically at
40 temperatures below 350°C, the near-surface cold work remained stable during high temperature

41 ⁶ The Full Width at Half Maximum (FWHM) intensity value of an x-ray diffraction peak often provides a reasonable
42 estimate of the degree of cold work (For instance, dislocation densities can roughly be estimated from FWHM-values
43 according to [50]). In addition, peak broadening is not only caused by strain (*e.g.*, micro-elastic inhomogeneous strain caused
44 by dislocations), but also by the size of the coherently scattering regions or domains in crystals. This means that
45 nanocrystallization causes additional broadening of Bragg diffraction peaks. However, a separation into strain- and (domain)
46 size-effects (*e.g.*, by profile analysis) was not performed in this study.

47 ⁷ This beneficial role of the nanocrystalline microstructure at the surface has been questioned in the literature [51] as fatigue
48 cracks may also form directly underneath such layers. However, as the stress-intensity factor developed ahead of a crack of a
49 given size is always larger for a surface crack than an internal crack, and any environmental (*e.g.*, corrosion) effects would be
50 greater for the surface crack, we still reason that the role of the nanocrystalline layer in suppressing surface crack initiation
51 and driving it sub-surface is highly beneficial to fatigue resistance.

1 fatigue up to 450°C; even at 550°C there was only a slight decrease of the FWHM-value after half the
2 number of cycles to failure.

3 4. Corresponding TEM studies of the surface regions of laser-shock peened samples fatigued at high
4 temperatures revealed dense and tangled dislocation arrangements just below the surface which were
5 quite stable under combined cyclic loading and elevated temperatures up to 350°C. Similarly, a region
6 of high dislocation density was also found in the deep-rolled condition in depths greater than 2 µm;
7 this region was found to be very stable during fatigue cycling at temperatures up to 350°C. In addition,
8 due to the severe and repeated plastic deformation as well as the 3-4 orders of magnitude lower strain
9 rate in deep-rolled compared to laser-peened structures [8], a nanocrystalline, 1-2 µm thick, surface
10 layer was formed after deep-rolling. TEM studies revealed that these nanocrystalline regions remained
11 unaffected in *thermomechanical* loading by the fatigue cycling at elevated temperature up to ~400°C.
12

13 5. Mechanistically, the main effect of such heavily dislocated nanoscale near-surface microstructures
14 appears to be in the suppression of surface crack initiation and early small crack growth, especially in
15 the HCF-regime. An observed decrease of broadening of x-ray diffraction peaks of deep-rolled
16 surface regions fatigued at 550°C suggest a rearrangement of dislocation structures into low-
17 energy/low lattice distortion networks at temperatures above 450°C. At temperatures below ~250°-
18 350°C, compressive residual stresses of about -400 MPa remain after cycling and are therefore
19 assumed to contribute significantly to lifetime extension due to the mechanical surface treatments.
20

21 6. Both surface treatments provide an effective means of fatigue life enhancement at all but very short
22 lives. Fatigue life enhancement is still in evidence up to ~250°-350°C as there is little significant
23 relaxation in surface compressive residual stresses and the near-surface work-hardened layers remain
24 stable. At T = 450°-550°C, however, the residual stresses have essentially completely relaxed but the
25 comparative stability of the work-hardened surface layers to both cyclic plasticity and temperature
26 lead to enhanced fatigue resistance (with a 50 MPa higher fatigue strength of deep-rolled or laser-
27 shock peened Ti-6Al-4V as compared to the untreated alloy) at 450° and 550°C.
28
29
30

31 **Acknowledgements**

32
33 This work was funded by the Deutsche Forschungsgemeinschaft (DFG) under grant numbers AL
34 558/1-2, 1-3 and 1-4. The involvement of ROR was supported by the Director, Office of Science,
35 Office of Basic Energy Sciences, Division of Materials Sciences and Engineering, of the U.S.
36 Department of Energy under Contract No. DE-AC02-05CH11231. The authors would like to thank
37 Mr. C. Rüppel, Dr. I. Nikitin and Dr. M. A. Cherif for their experimental assistance.
38
39
40

41 **References**

- 42
43
44 [1] Helm D. Application of Ti-Alloys as compressor discs and blades. In: Boyer RR, Eylon D,
45 Lütjering G, editors. *Fatigue Behavior of Titanium Alloys*, TMS, Warrendale (USA), 1999, pp.
46 291-98.
47
48 [2] Traiser H, Kloos KH. Einfluß einer Oberflächenkaltverfestigung auf die Schwingfestigkeit und
49 das Wechselverformungsverhalten der normalisierten Kohlenstoffstähle Ck 15 und Ck 45 unter
50 Zugdruck-und Umlaufbiegebeanspruchung. *Z. Werkstofftech.*, 1985;**16**: 135-43.
51
52 [3] Schulze V, Lang KH, Vöhringer O, Macherauch E. Relaxation of shot peening induced residual
53 stresses in quenched and tempered steel AISI 4140 due to uniaxial cyclic deformation In:
54 Champaigne J, editor. *Proc. 6th Int. Conf. on Shot Peening (ICSP6)*, San Francisco, 1996, pp.
55 403-12.
56
57 [4] Ebenau A, Vöhringer O, Macherauch E, Eifler D. Influence of shot peening on the cyclic
58 deformation behaviour of the steel 42CrMo4 in a normalized state. In: Iida K, editor. *Proc. 4th*
59 *Int. Conf. on Shot Peening (ICSP4)*, Tokyo, 1990, pp. 327-336.
60
61
62
63
64
65

- 1 [5] Juijerm P, Altenberger I. Cyclic deformation behavior and its optimization at elevated
2 temperature. In: Kvackaj T, editor. Aluminium Alloys, Theory and Applications, InTech, 2011,
3 pp. 183-198.
4
- 5 [6] Lukas P, Klesnil M, Polak J. High cycle fatigue life of metals. *Mater. Sci. Eng.*, 1974;**15**:239-
6 45.
7
- 8 [7] Gray H, Wagner L, Lütjering G. Influence of shot peening on the fatigue strength of Ti-alloys at
9 elevated temperatures. In: Barnby JT, editor. Fatigue Prevention and Design, Chamelion Press,
10 London UK, 1986, pp. 363-76.
11
- 12 [8] Altenberger I. Alternative mechanical surface treatments – microstructure, residual stresses and
13 fatigue behaviour. In: Wagner L, editor, Shot Peening, Wiley-VCH, ICSP8, Garmisch-
14 Partenkirchen, pp. 421-34.
15
- 16 [9] Wagner L, Ludian T, Wollmann M. Ball-burnishing and roller-burnishing to improve fatigue
17 performance of structural alloys, In: Pantelakis S, Rodopoulos C, editors. Engineering against
18 Fracture, Springer Science+Business Media B.V., 2009, pp.1-11.
19
- 20 [10] Prevey PS, Jayaraman N, Cammett J. Overview of low plasticity burnishing for mitigation of
21 fatigue damage mechanisms, In: Schulze V, Niku-Lari A, editors. Proc. 9th Intl. Conf. on Shot
22 Peening (ICSP9), IITT International, Paris, 2005, pp. 267-72.
23
- 24 [11] Hill MR, Pistochini TE, DeWald AT. Optimization of residual stress and fatigue life in laser
25 peened components. In: Schulze V, Niku-Lari A, editors. Proc. 9th Intl. Conf. on Shot Peening
26 (ICSP9), IITT International, Paris, 2005, pp. 156-62.
27
- 28 [12] Montross CS, Wei T, Ye L, Clark G, Mai YW. Laser shock processing and its effects on
29 microstructure and properties of metal alloys: a review. *Int. J. Fatigue*, 2002;**24**:1021-36.
30
- 31 [13] Yang JM, Her YC, Han N, Clauer A. Laser shock peening on fatigue behavior of 2024-T3 Al
32 alloy with fastener holes and stopholes. *Mater. Sci. Eng. A*, 2001;**298**:296-99.
33
- 34 [14] Peyre P, Fabbro R, Merrien P, Lieurade HP Laser shock processing of aluminium alloys.
35 Application to high cycle fatigue behaviour. *Mater. Sci. Eng. A*, 1996;**210**:102-13.
36
- 37 [15] Gray H, Wagner L, Lütjering G. Influence of shot peening induced surface roughness, residual
38 macrostresses and dislocation density on the elevated temperature HCF-properties of Ti-alloys.
39 In: Wohlfahrt H, editor. Shot Peening, DGM, 1987, pp. 447-58.
40
- 41 [16] Ludian T, Wagner L. Mechanical surface treatments for improving fatigue behaviour in titanium
42 alloys. *Advances in Materials Science*, 2008;**8**:44-52.
43
- 44 [17] Cherif MA, Knobbe H, Altenberger I, Krupp U, Near-surface characteristics and fatigue
45 behavior of laser shock peened titanium alloy Timetal LCB. In: Niinomi M, Akiyama S,
46 Hagiwara M, Ikeda M, Maruyama K, editors. Ti-2007 Science and Technology (Proc. 11th
47 World Titanium Conference), Kyoto, 2007, pp. 1667-71.
48
- 49 [18] Nalla RK, Altenberger I, Noster U, Liu GY, Scholtes B, Ritchie RO. On the influence of
50 mechanical surface treatments -deep rolling and laser shock peening- on the fatigue behavior of
51 Ti-6Al-4V at ambient and elevated temperatures. *Mater. Sci. Eng. A*, 2003;**355**:216-30.
52
- 53 [19] Wagner L. Mechanical surface treatments on titanium, aluminum and magnesium alloys, *Mater.*
54 *Sci. Eng. A*. 1999;**263**:210-16.
55
56
57
58
59
60
61
62
63
64
65

- 1 [20] Wagner L, Mhaede M, Wollmann M, Altenberger I, Sano Y. Surface layer properties and
2 fatigue behavior in Al 7075-T73 and Ti-6Al-4V: Comparing results after laser peening; shot
3 peening and ball-burnishing. *Int. J. of Struct. Integrity*, 2011;**2**:185-99.
- 4 [21] Altenberger I, Noster U, Boyce BL, Peters JO, Scholtes BO, Ritchie RO. Effects of mechanical
5 surface treatment on fatigue failure in Ti-6Al-4V: Role of residual stresses and foreign-object
6 damage. *Mater. Sci. Forum*, 2002;**404-407**:457-62.
- 7 [22] Altenberger I, Stach EA, Liu G, Nalla RK, Ritchie RO. An in situ transmission electron
8 microscope study of the thermal stability of near-surface microstructures induced by deep
9 rolling and laser-shock peening. *Scripta Materialia*, 2003;**48**:593-98.
- 10 [23] Peters JO, Ritchie RO. Influence of foreign-object damage on crack initiation and early crack
11 growth during high-cycle fatigue of Ti-6Al-4V. *Eng. Fract. Mech.*, 2000;**67**:193-207.
- 12 [24] Ritchie RO, Boyce BL, Campbell JP, Roder O, Thompson AW, Milligan WW. Thresholds for
13 high-cycle fatigue in a turbine engine Ti-6Al-4V alloy. *Int. J. Fatigue*, 1999;**21**:653-62.
- 14 [25] Boyce BL, Ritchie RO. Effect of load ratio and maximum stress intensity on the fatigue
15 threshold in Ti-6Al-4V. *Eng. Fract. Mech.*, 2001;**68**:129-47.
- 16 [26] Nalla RK, Boyce BL, Campbell JP, Peters JO, Ritchie RO. Influence of microstructure on high-
17 cycle fatigue of Ti-6Al-4V: Bimodal vs. lamellar structures. *Metall. Mater. Trans. A*,
18 2002;**33A**:899-918.
- 19 [27] Sano Y, Obata M, Kubo T, Mukai N, Yoda M, Masaki K, Ochi Y. Retardation of crack
20 initiation and growth in austenitic stainless steels by laser peening without protective coating.
21 *Mater. Sci. Eng A*, 2006;**417**:334-40.
- 22 [28] Macherauch E, Müller P. Das $\sin^2\psi$ -Verfahren der röntgenographischen Spannungsmessung. *Z.*
23 *f. angew. Physik*, 1961;**13**:305-12.
- 24 [29] Altenberger I, Scholtes B, Martin U, Oettel H. Cyclic deformation and near surface
25 microstructures of shot peened or deep rolled austenitic stainless steel AISI 304. *Mater. Sci.*
26 *Eng. A*, 1999;**264**:1-16.
- 27 [30] Moelle CH, Fecht HJ. Thermal stability of nanocrystalline iron prepared by mechanical attrition.
28 *Nanostructured Materials*, 1995;**6**:421-24.
- 29 [31] Hanagarth H. Auswirkungen von Oberflächenbehandlungen auf das Ermüdungs-
30 verhalten von TiAl6V4 und 42CrMo4 bei erhöhter Temperatur. Dr.-Ing. Thesis, University Karlsruhe (TH),
31 1989.
- 32 [32] Altenberger I, Sano Y, Nikitin I, Scholtes B. Fatigue behavior and residual stress state of laser
33 shock peened materials at ambient and elevated temperatures. In: Fatigue 2006, Proc. 9th Int.
34 Fatigue Congress, 2006, Elsevier Ltd., paper FT124.
- 35 [33] Pollak RD. Analysis of methods for determining high cycle fatigue strength of a material with
36 investigation of titanium-aluminum-vanadium gigacycle fatigue behaviour. Ph.D. Thesis, Air
37 Force Institute of Technology, Air University, 2005.
- 38 [34] McClung RC. A literature survey on the stability and significance of residual stresses during
39 fatigue. *Fatigue Fract. Engng. Mater. Struct.*, 2007;**30**:173-205.
- 40 [35] Juijerm P, Altenberger I. Cyclic deformation behavior of deep rolled as-quenched aluminium
41 alloy AA6110 at elevated temperatures. *Int. J. Mat. Res.*, 2007;**98**:506-10.
- 42
43
44
45
46
47
48
49
50
51
52
53
54
55
56
57
58
59
60
61
62
63
64
65

- 1 [36] Schulze V. Modern Mechanical Surface Treatments. Wiley-VCH, 2005.
- 2
- 3 [37] John R, Buchanan DJ, Jha SK, Larsen JM. Stability of shot-peen residual stresses in an $\alpha + \beta$
- 4 titanium alloy. *Scripta Mater.*, 2009;**61**:343-46.
- 5
- 6 [38] Juijerm P, Altenberger I. Effective boundary of deep-rolling treatment and its correlation with
- 7 residual stress stability of Al–Mg–Mn and Al–Mg–Si–Cu alloys. *Scripta Mater.*, 2007;**56**:745-
- 8 48.
- 9
- 10 [39] Schwilling B, Fleck C, Eifler D. Cyclic deformation behaviour of TiAl6V4 and TiAl6Nb7 in
- 11 different quasi-physiological media. *Mater. wiss. u. Werkstofftech.*, 2002;**33**:453-58.
- 12
- 13 [40] Marmy P, Leguey T, Belianov I, Sauder M, Brüttsch R. unpublished work, 2003.
- 14
- 15 [41] Marmy P, Leguey T, Belianov I, Victoria M. Tensile and fatigue properties of two titanium
- 16 alloys as candidate materials for fusion reactors. *Journal of Nuclear Materials*, 2000;**283-**
- 17 **287**:602-06.
- 18
- 19 [42] Leguey T, Schäublin R, Marmy P, Victoria M. Microstructure of Ti5Al2.5Sn and Ti6Al4V
- 20 deformed in tensile and fatigue tests. *Journal of Nuclear Materials*, 2002; **305**:52-59.
- 21
- 22 [43] Berling JT, Slot T. Effect of temperature and strain rate on low-cycle fatigue resistance of AISI
- 23 304, 316 and 348 stainless steel. In: ASTM Spec. Tech. Pub. 459 (1969), pp. 3-30.
- 24
- 25 [44] Lukas P, Kunz L. Effect of low temperatures on the cyclic stress-strain response and high cycle
- 26 fatigue life of polycrystalline copper. *Mater. Sci. Eng. A*, 1998;**103**:233-39.
- 27
- 28 [45] Noster U, Altenberger I, Scholtes B. Isothermal fatigue of magnesium wrought alloy AZ 31. In:
- 29 Kainer KU, editor. Proc. Magnesium Alloys and their Applications, Verlag Wiley-VCH,
- 30 Weinheim, 2000, pp. 312-17.
- 31
- 32 [46] Martin U, Altenberger I, Scholtes B, Kremmer K, Oettel H. Cyclic deformation and near
- 33 surface microstructures of normalized shot peened steel SAE 1045. *Mater. Sci. Eng. A*,
- 34 1998;**246**:69-80.
- 35
- 36 [47] Padilla II HA, Boyce BL. A review of fatigue behavior in nanocrystalline metals, *Exp.*
- 37 *Mechanics*. 2010;**50**:5-23.
- 38
- 39 [48] Juijerm P, Altenberger I, Noster U, Scholtes B. Residual stress relaxation and cyclic
- 40 deformation behavior of deep rolled AlMg4.5Mn (AA5083) at elevated temperatures. *Mater.*
- 41 *Sci. Forum*, 2005;**490**:436-41.
- 42
- 43 [49] Juijerm P, Altenberger I. Residual stress relaxation of deep-rolled Al–Mg–Si–Cu alloy during
- 44 cyclic loading at elevated temperatures. *Scripta Mater.*, 2006;**55**:1111-14.
- 45
- 46 [50] Williamson GK, Smallman RE. Dislocation densities in some annealed and cold-worked metals
- 47 from measurements on the X-ray Debye-Scherrer spectrum. *Phil. Mag.*, 1956;**1**:34-46.
- 48
- 49 [51] Altenberger I, Scholtes B, Noster U, Ritchie RO, Characterization of fatigue crack formation in
- 50 mechanically surface treated austenitic stainless steel. In: Ravi-Chandar K, Karihaloo BL, Kishi
- 51 T, Ritchie RO, Yokobori AT, Okobori T, editors. Advances in Fracture Research – Proc. Intl.
- 52 Conf. on Fracture 10, Honolulu 2001, Elsevier Science, UK, 2001.
- 53
- 54 [52] Ruschau JJ, John R, Thompson SR, Nicholas T. Fatigue crack nucleation and growth rate
- 55 behavior of laser shock peened titanium. *Int. J. Fatigue*, 1999;**21**:S199-S209.
- 56
- 57
- 58
- 59
- 60
- 61
- 62
- 63
- 64
- 65

- 1 [53] Röttger K, Wilcke G, Altenberger I, Festwalzen hochbeanspruchter Bauteile zur Steigerung der
2 Festigkeit. In: DVM-Bericht 131 "Leichtbau und Betriebsfestigkeit“, München, 2004, pp. 293-
3 302.
4
- 5 [54] Peters JO, Lütjering G, Nalla RK, Altenberger I, Ritchie RO. High cycle fatigue of beta-
6 titanium alloys, in: Fatigue 2002, Proceedings of the Eighth International Fatigue Congress,
7 Blom AF, editor, EMAS, Cradley Heath, West Midlands, UK, 2002, vol. 3, pp. 1763-72.
8
9

10
11
12
13
14
15
16
17
18
19
20
21
22
23
24
25
26
27
28
29
30
31
32
33
34
35
36
37
38
39
40
41
42
43
44
45
46
47
48
49
50
51
52
53
54
55
56
57
58
59
60
61
62
63
64
65

LIST OF TABLE CAPTIONS

Table 1: Manson-Coffin slopes b of the regressions in Fig. 6. Corresponding equation for the Manson-Coffin regression: $y = a \cdot x^b$.

LIST OF FIGURE AND TABLE CAPTIONS

Fig. 1: Optical micrograph of the microstructure of the bimodal Ti-6Al-4V (solution treated and overaged) alloy, showing interconnected equiaxed primary α -grains (light colored) interdispersed within $\alpha+\beta$ (transformed β) colonies (grey-lamellar like). Sample was etched for ~ 10 s in Kroll solution), *i.e.*, five parts 70% HNO₃, ten parts 50% HF, and 85 parts of H₂O.

Fig. 2: Bright-field TEM-micrographs of the near-surface microstructures of the annealed (a), deep-rolled (b) and laser-shock-peened (c) condition showing the typical work hardening state of surface regions before (a) and after mechanical surface treatment (b and c) (distance to surface 0-2 μm , perspective: not cross-sectional, but plan view).

Fig. 3: S/N fatigue curves at $R = -1$ for Ti-6Al-4V at room temperature for the annealed (non-surface treated), laser-shock peened and deep-rolled surface treated materials.

Fig. 4: S/N fatigue curves at $R = -1$ for Ti-6Al-4V at 250°C (a), 350°C (b), 450°C (c) and 550°C (d) for the annealed (non-surface treated), laser-shock peened and deep-rolled surface treated materials.

Fig. 5: Cyclic softening curves at different stress amplitudes for isothermally fatigued Ti-6Al-4V at 250°C ((a) and (b)) and 350°C ((c) and (d)) in the untreated ((a) and (c)) and in the deep-rolled ((b) and (d)) conditions.

Fig. 6: Manson-Coffin-plot for deep-rolled and untreated Ti-6Al-4V at room temperature and elevated temperature.

Fig. 7: TEM micrographs of the nanocrystalline surface regions and sub-surface regions (5 μm below the surface) of deep-rolled Ti-6Al-4V after stress-controlled high-temperature fatigue at 200°C and at 400°C. Samples were cycled at a stress amplitude of 430 MPa for 2,000 cycles. In view of Figs. 2 and 7, it is evident, that the nanocrystalline surface region, as well as the highly work hardened sub-surface region exhibiting a highly tangled dislocation arrangement, remained stable during high-temperature fatigue at both temperatures at this stress amplitude.

Fig. 8: Surface regions of laser-shock peened (with coating) Ti-6Al-4V after stress-controlled high-temperature fatigue at 250°C (a) and 350°C (b). Samples were cycled at a stress amplitude of 460 MPa for 50,000 and 18,000 cycles, respectively (equivalent to $N_f/2$) (TEM micrograph)

Fig. 9: SEM micrographs (using secondary electrons) of the fracture surfaces of untreated (a) and of deep-rolled Ti-6Al-4V (b) (stress amplitude 540 MPa at 250°C). (c) SEM micrograph (using secondary electrons) of the fracture surface of untreated Ti-6Al-4V (stress amplitude 370 MPa at 550°C). (Arrow in (c) indicates the general direction of crack propagation).

1 **Fig. 10:** Fatigue strength of untreated and deep-rolled Ti-6Al-4V as a function of test
2 temperature at 10^6 cycles to failure ($R = -1$, 5 Hz frequency).

3
4 **Fig. 11:** Residual stress relaxation at the surface of deep-rolled specimens during stress-
5 controlled fatigue (at a stress amplitude 460 MPa) at different isothermal fatigue
6 temperatures.

7
8 **Fig. 12:** Peak-broadening of x-ray diffraction peaks (FWHM-values) at the surface of deep-
9 rolled specimens during stress-controlled fatigue (at a stress amplitude 460 MPa) at different
10 isothermal fatigue temperatures.
11
12
13
14
15
16
17
18
19
20
21
22
23
24
25
26
27
28
29
30
31
32
33
34
35
36
37
38
39
40
41
42
43
44
45
46
47
48
49
50
51
52
53
54
55
56
57
58
59
60
61
62
63
64
65

Table 1: Manson-Coffin slopes b of the regressions in Fig. 6. Corresponding equation for the Manson-Coffin regression: $y = a \cdot x^b$.

	b	a
untreated condition, 22°C	-0.76	77.18
untreated condition, 550°C	-0.96	408.89
deep rolled condition, 22°C	-0.61	34.47
deep rolled condition, 550°C	-0.47	12.67
untreated condition, 22°C	-0.67	25.17

Figure 1
[Click here to download high resolution image](#)

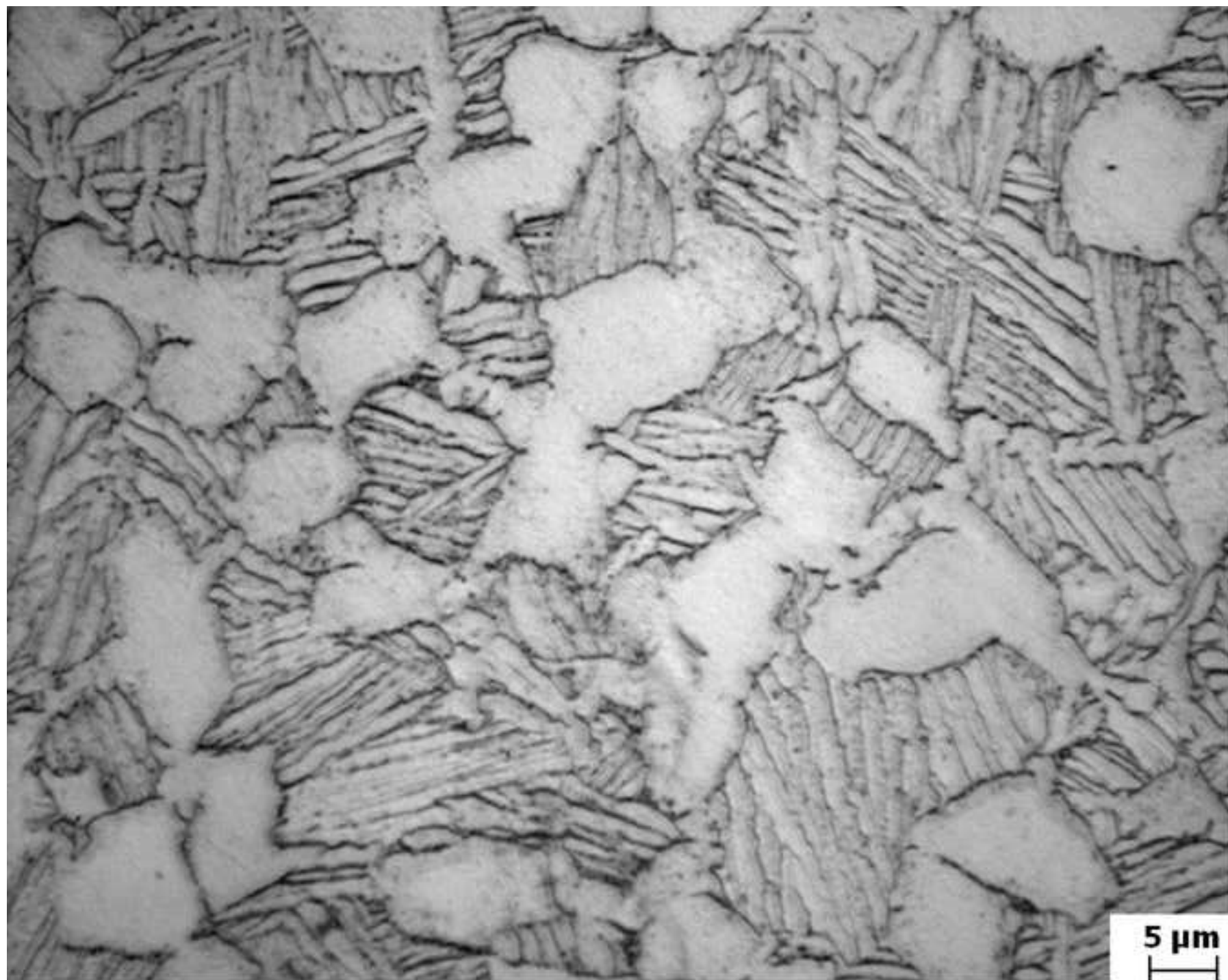


Figure 2
[Click here to download high resolution image](#)

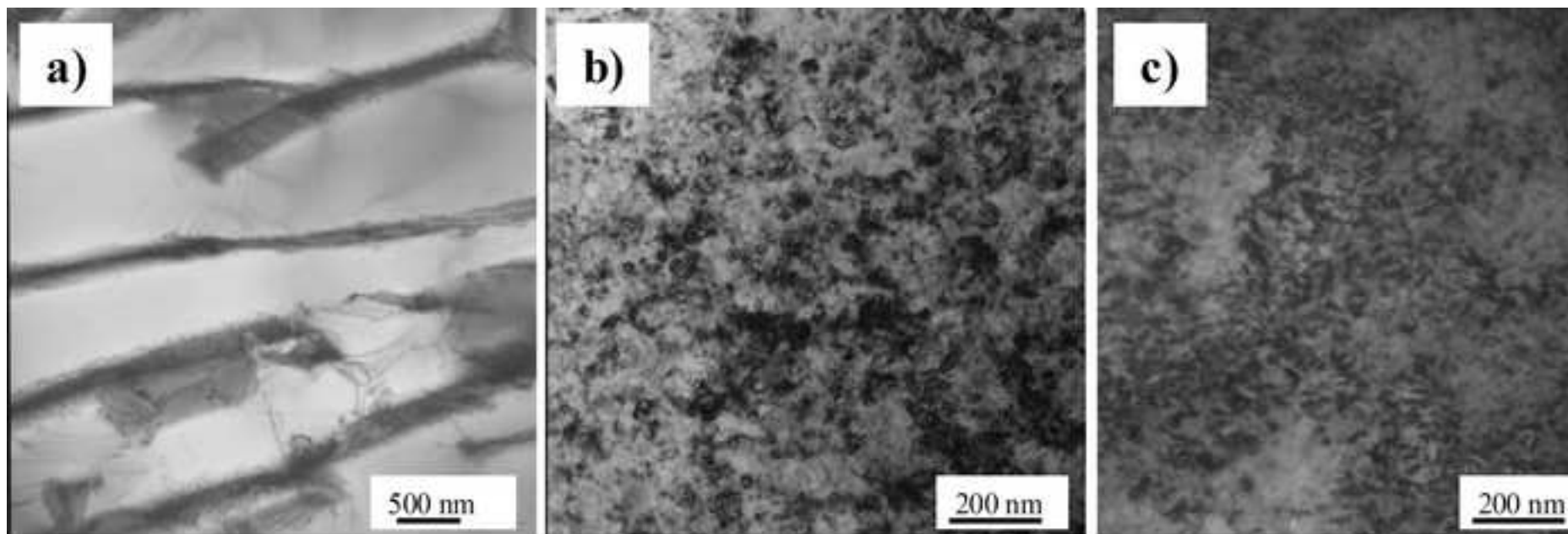


Figure 3

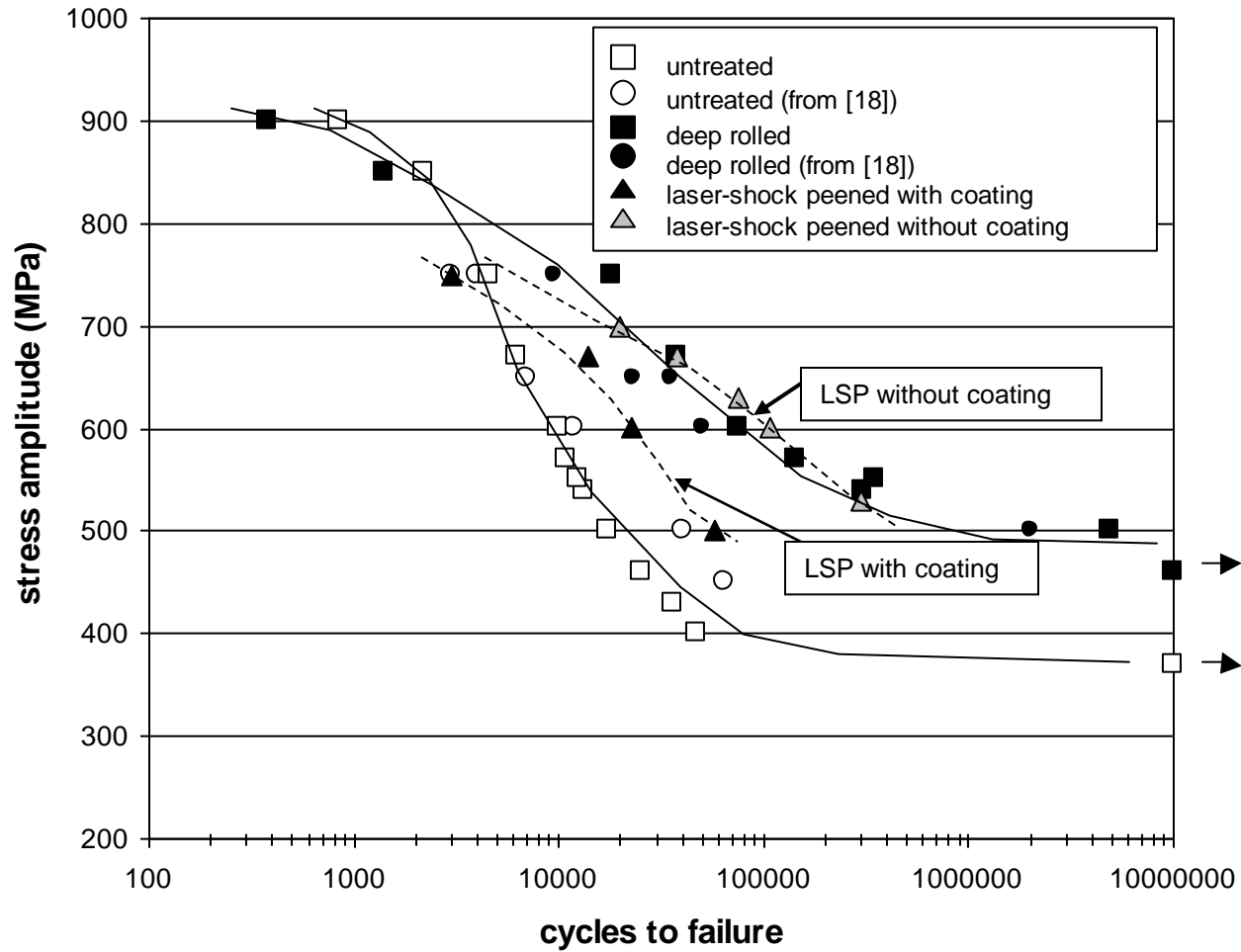


Figure 4
[Click here to download high resolution image](#)

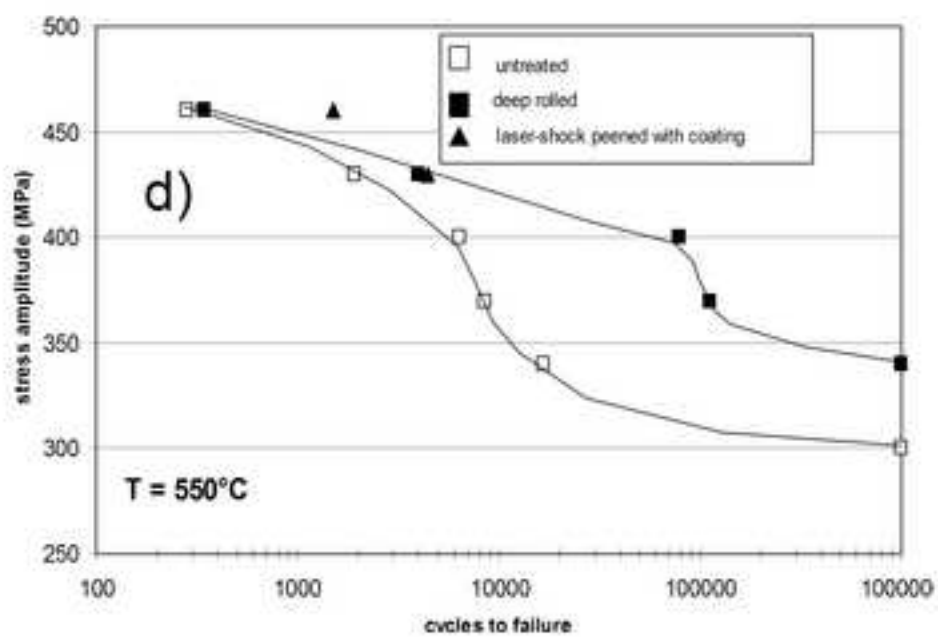
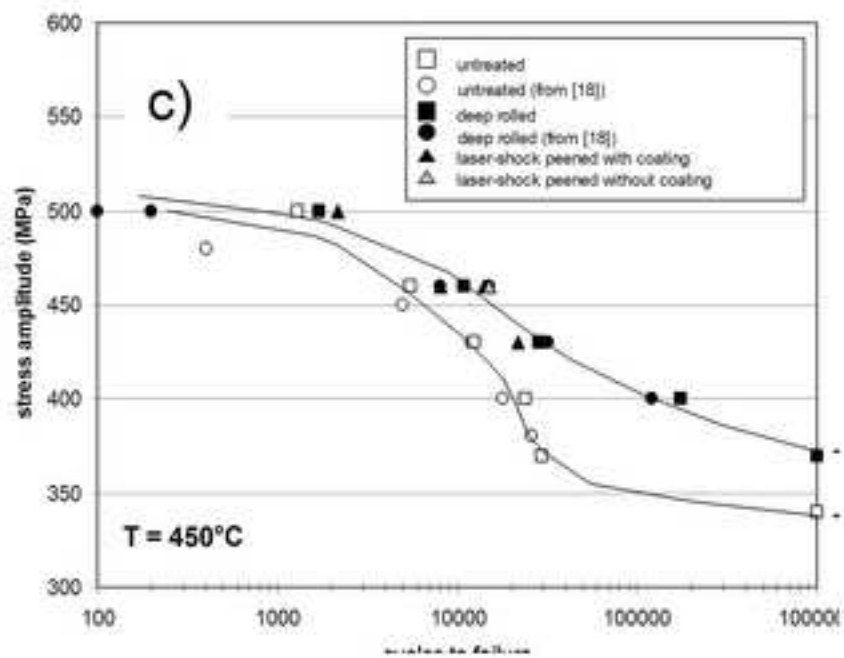
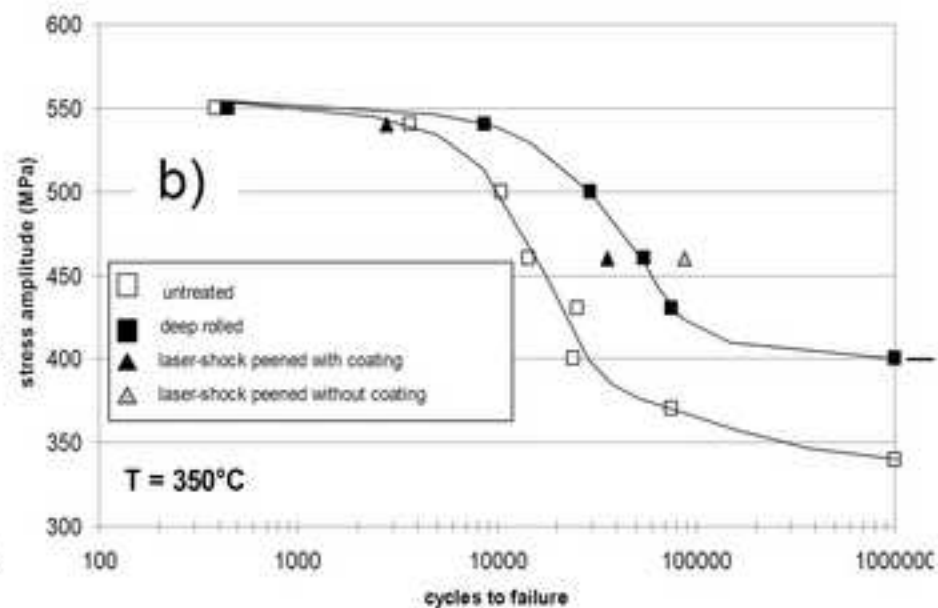
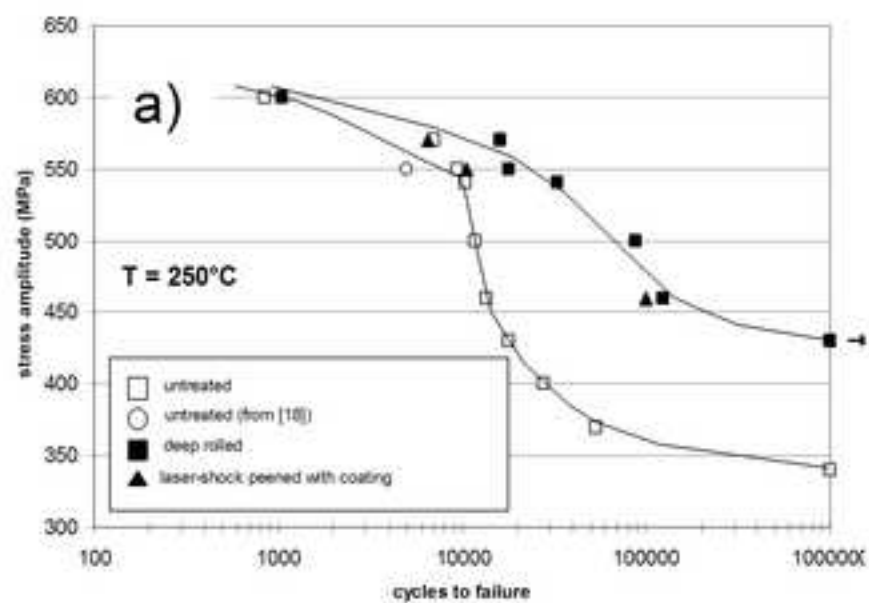


Figure 5
[Click here to download high resolution image](#)

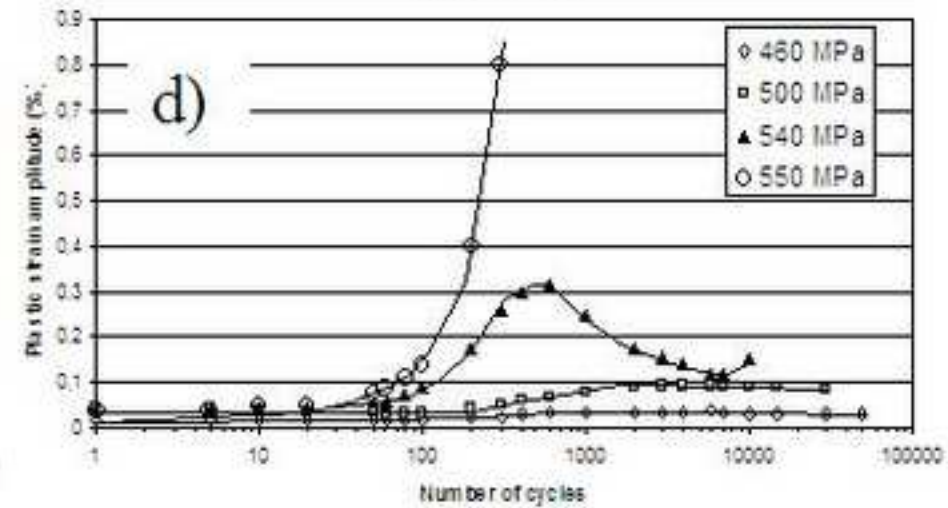
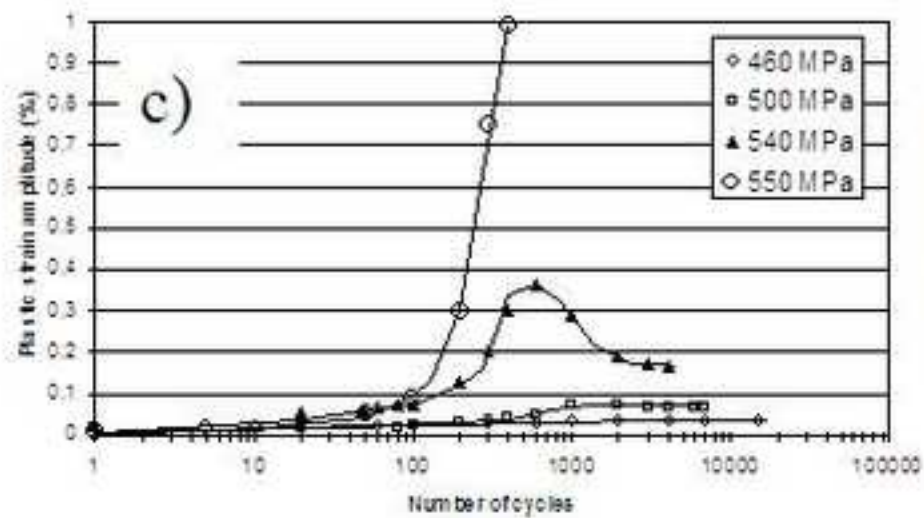
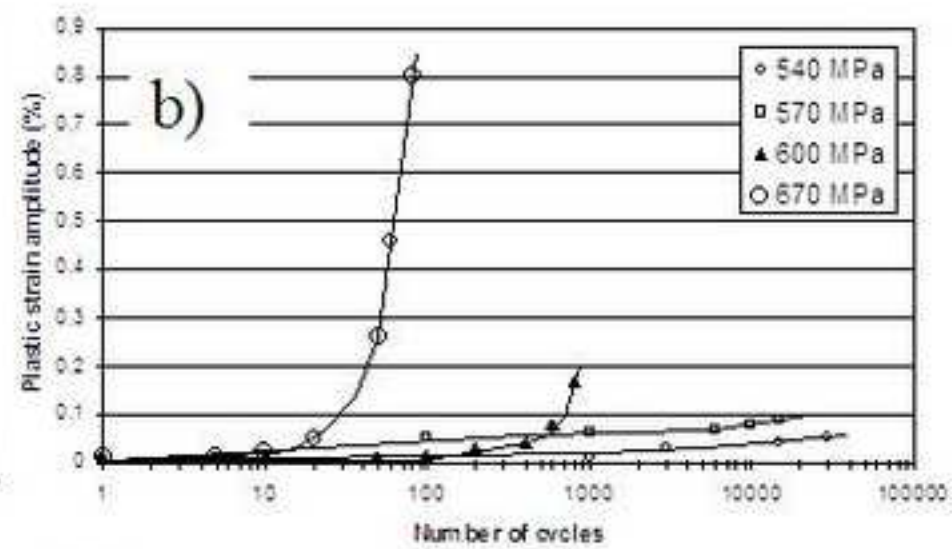
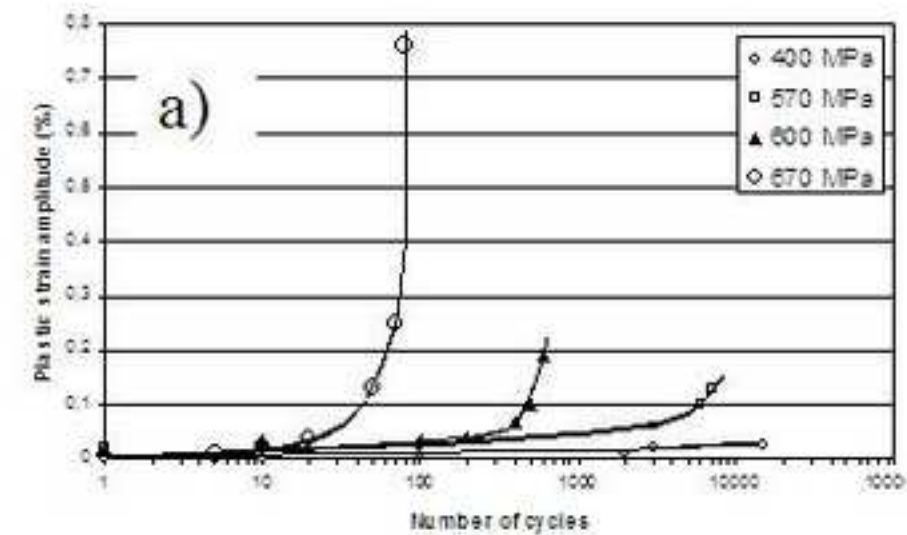


Figure 6

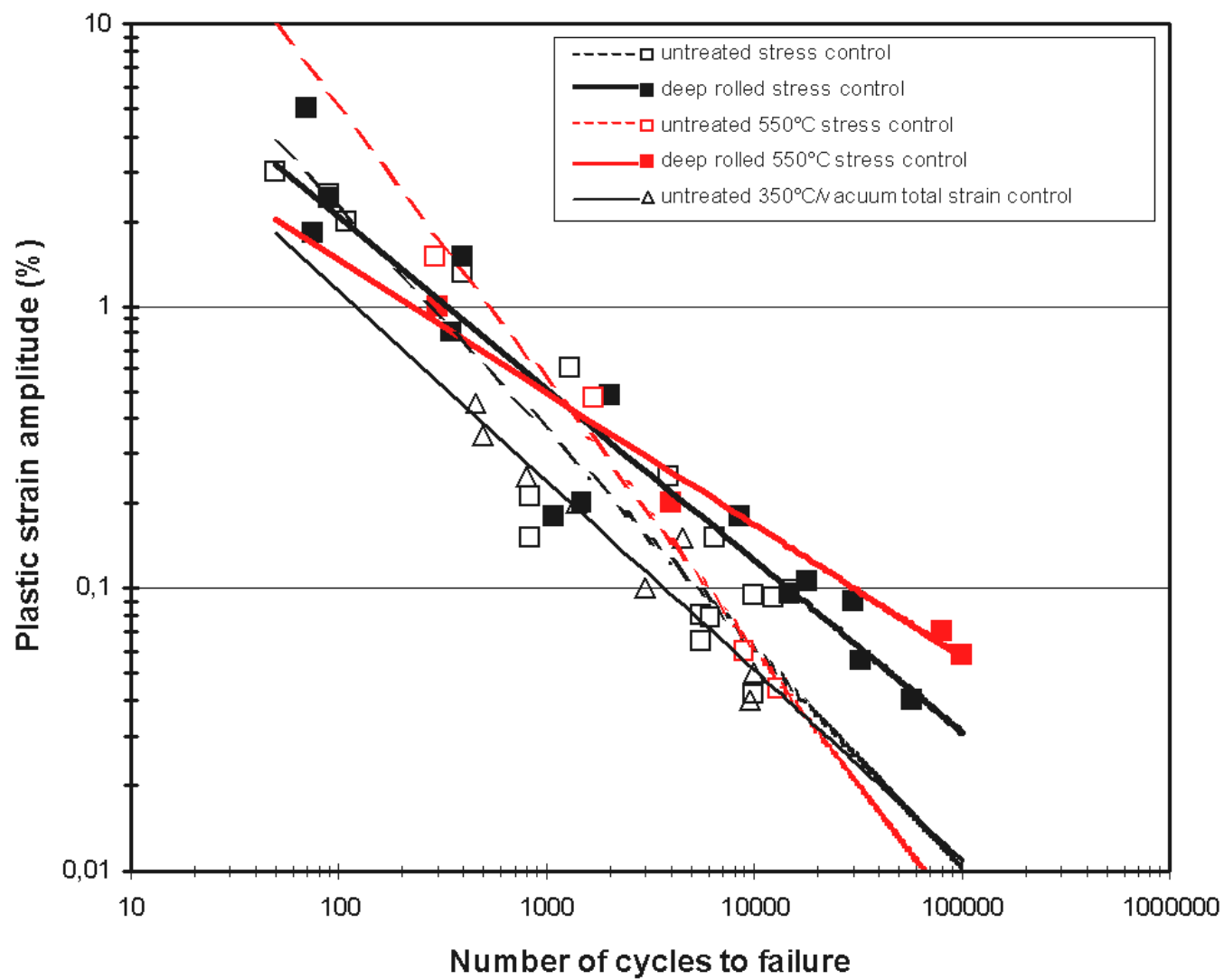
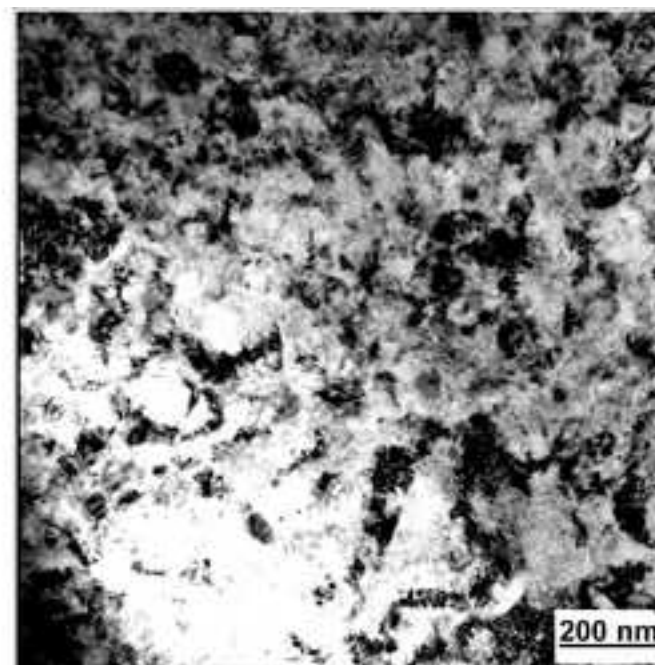
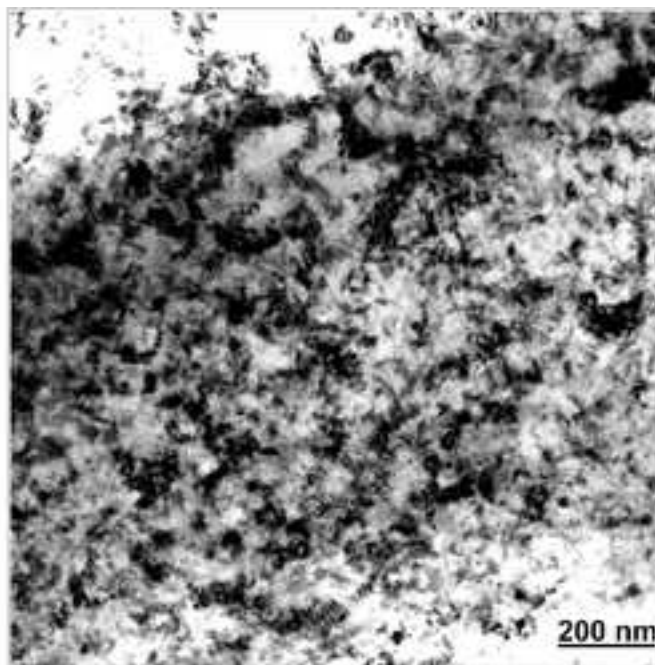
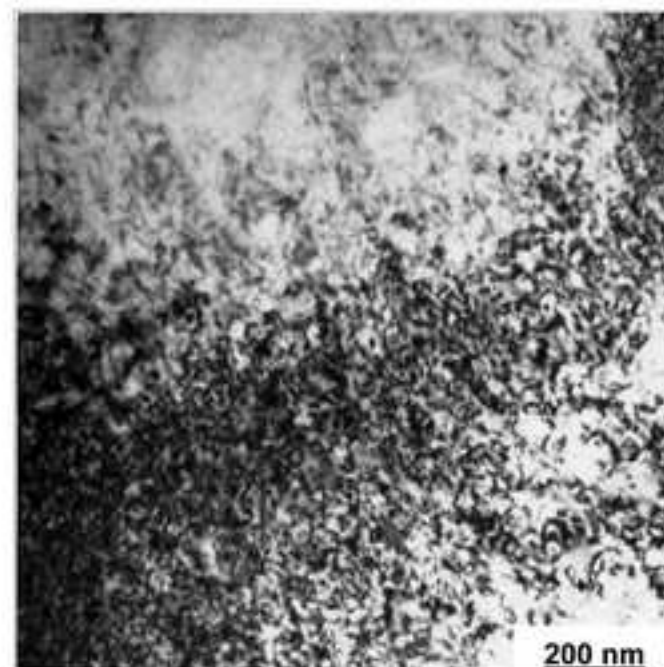
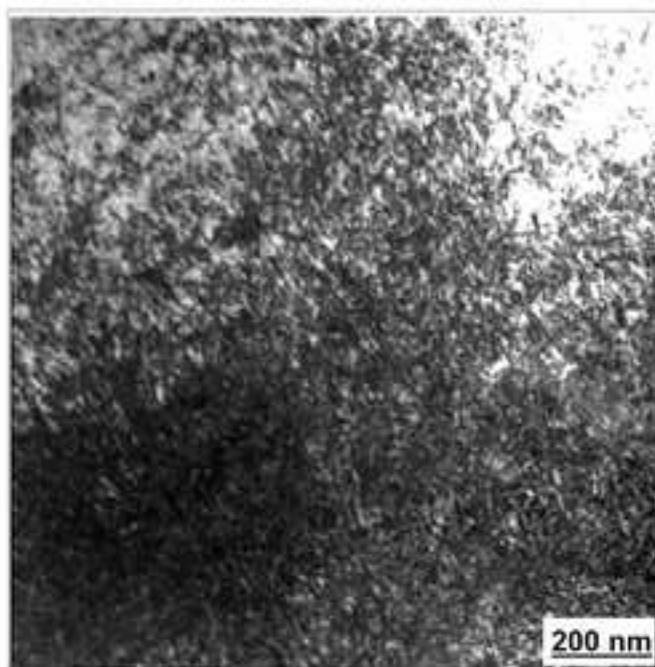


Figure 7
[Click here to download high resolution image](#)

surface



5 μm depth



200°C

400°C

Figure 8
[Click here to download high resolution image](#)

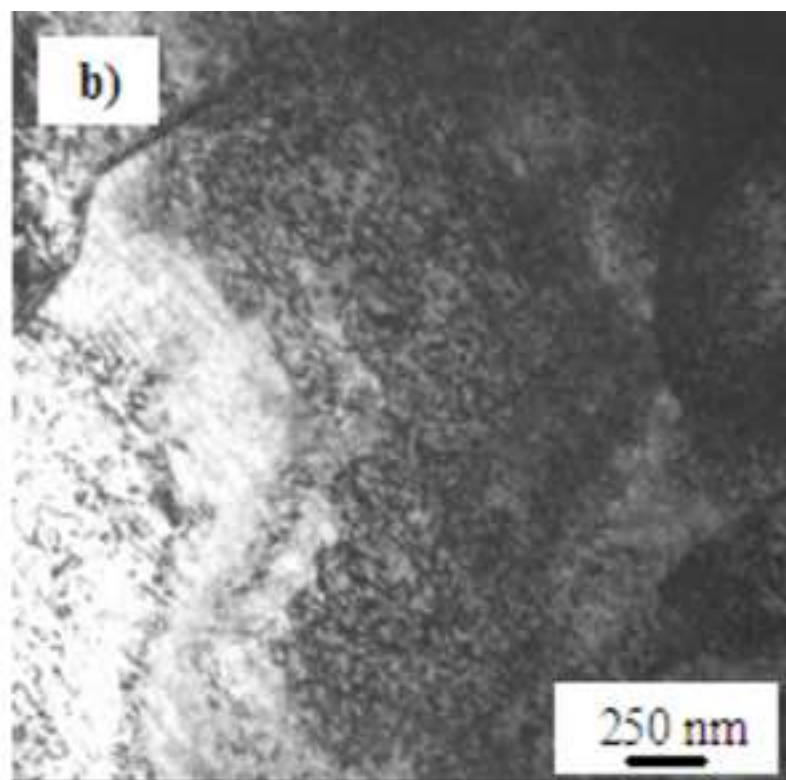
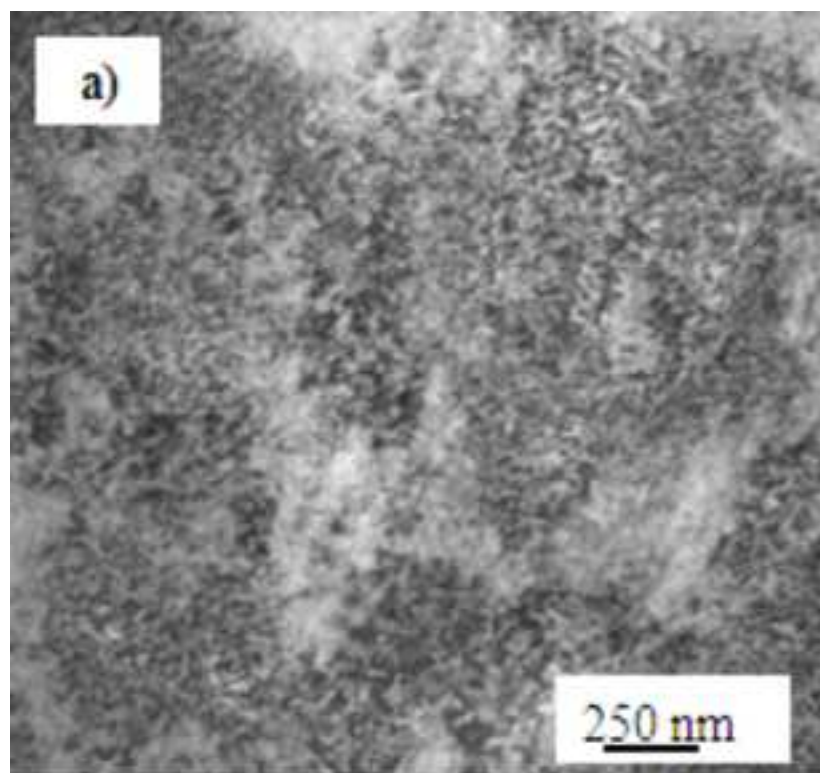


Figure 9
[Click here to download high resolution image](#)

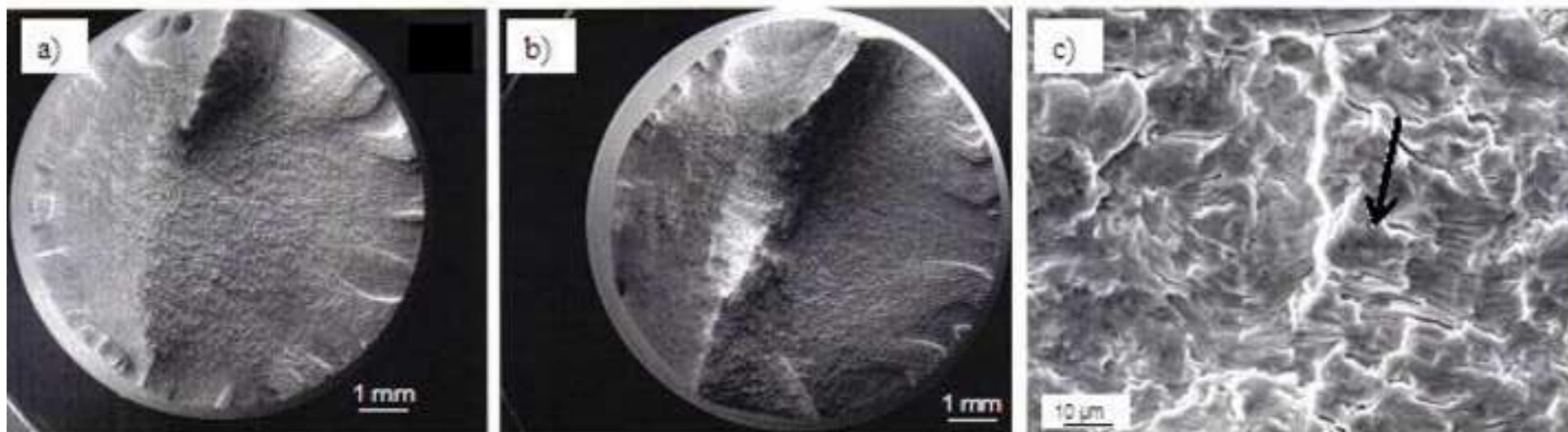


Figure 10
[Click here to download high resolution image](#)

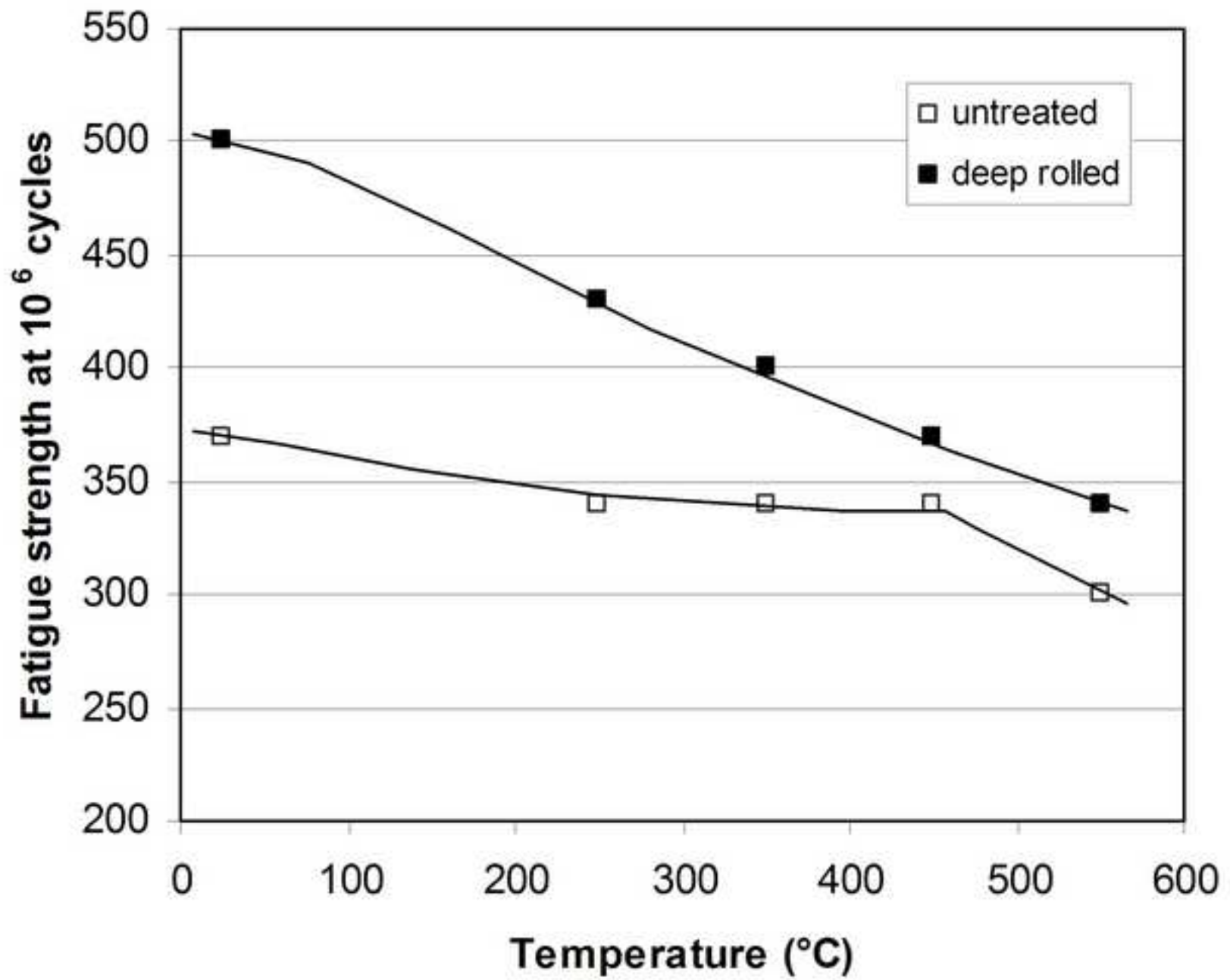


Figure 11
[Click here to download high resolution image](#)

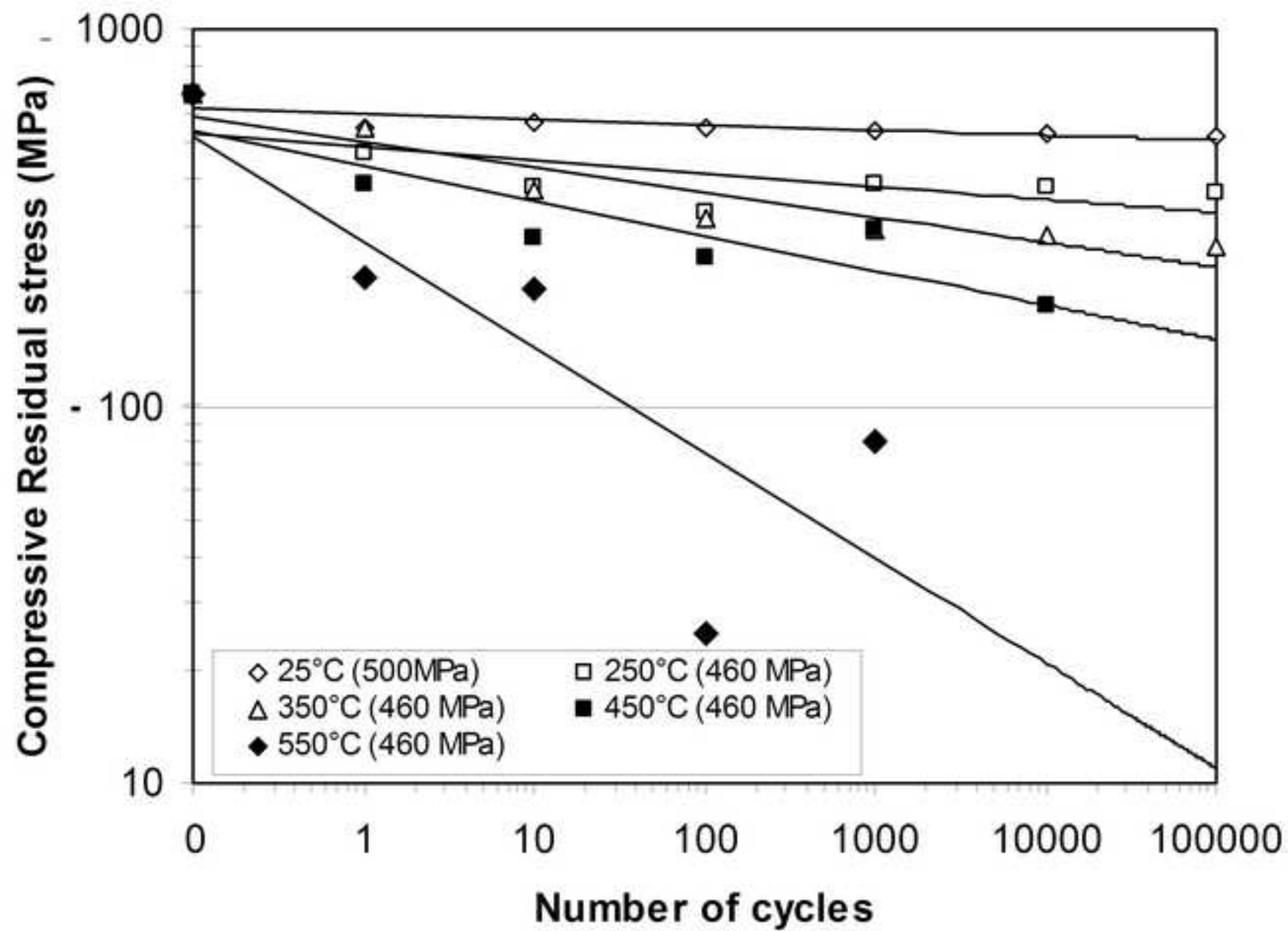
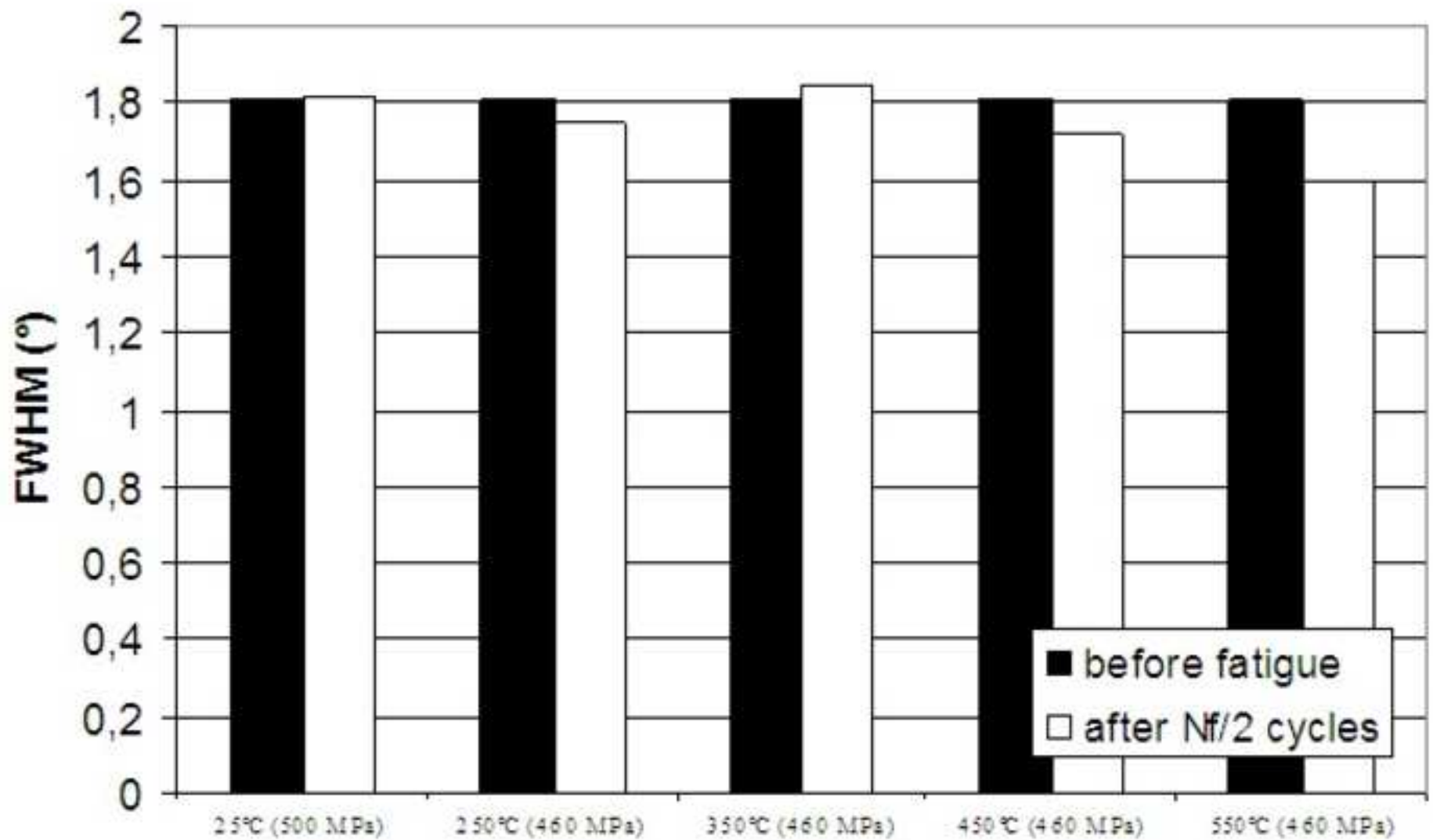


Figure 12
[Click here to download high resolution image](#)



DISCLAIMER

This document was prepared as an account of work sponsored by the United States Government. While this document is believed to contain correct information, neither the United States Government nor any agency thereof, nor the Regents of the University of California, nor any of their employees, makes any warranty, express or implied, or assumes any legal responsibility for the accuracy, completeness, or usefulness of any information, apparatus, product, or process disclosed, or represents that its use would not infringe privately owned rights. Reference herein to any specific commercial product, process, or service by its trade name, trademark, manufacturer, or otherwise, does not necessarily constitute or imply its endorsement, recommendation, or favoring by the United States Government or any agency thereof, or the Regents of the University of California. The views and opinions of authors expressed herein do not necessarily state or reflect those of the United States Government or any agency thereof or the Regents of the University of California.